Best theory diagrams for cross-ply composite plates using polynomial, trigonometric and exponential thickness expansions

(Article begins on next page)

10 April 2025

Best Theory Diagrams for Cross-Ply Composite Plates using Polynomial, Trigonometric and Exponential Thickness Expansions

J. Yarasca [a], J. L. Mantari [a], M. Petrolo [b], E. Carrera [b]

a Faculty of Mechanical Engineering, Universidad de Ingeniería y Tecnología (UTEC), Medrano Silva 165, Barranco, Lima, Peru

b Department of Mechanical and Aerospace Engineering, Politecnico di Torino, Corso Duca degli Abruzzi 24, 10129 Torino, Italy

Best Theory Diagrams for Cross-Ply Composite Plates using Polynomial, Trigonometric and Exponential Thickness Expansions

This paper presents Best Theory Diagrams (BTDs) employing combinations of Maclaurin, trigonometric and exponential terms to build two-dimensional theories for laminated cross-ply plates. The BTD is a curve in which the least number of unknown variables to meet a given accuracy requirement is read. The used refined models are Equivalent Single Layer and are obtained using the Unified Formulation developed by Carrera. The governing equations are derived from the Principle of Virtual Displacement (PVD), and Navier-type closed form solutions have been obtained in the case of simply supported plates loaded by a bisinuisoidal transverse pressure. BTDs have been constructed using the Axiomatic/Asymptotic Method (AAM) and genetic algorithms (GA). The influence of trigonometric and exponential terms in the BTDs has been studied for different layer configurations, length-to-thickness ratios and stresses. It is shown that the addition of trigonometric and exponential expansion terms to Maclaurin ones may improve the accuracy and computational cost of refined plate theories. The combined use of CUF, AAM and GA is a powerful tool to evaluate the accuracy of any structural theory.

Keywords: Plates; Carrera Unified Formulation (CUF); Trigonometric; Exponential; Best Theory Diagram; Composite Structures.

1. Introduction

Laminated composite plates are extensively used in many engineering applications due to their high strength-to-weight ratio, high stiffness-to weight ratio, environmental resistance and the ability to tailor properties for desired applications. An accurate analysis of composite structures is fundamental for a reliable structural design. Several researchers have investigated the modelling of the laminated composites over the past few decades and some structural models have been developed for their analysis.

Classical plate theories (CPT), originally developed for thin isotropic plates [1, 2], neglect transverse shear and normal stresses. An extension of this model to multi-

layered structures is referred to as the Classical Lamination Theory (CLT) [3, 4]. Reissner and Mindlin [5, 6] included transverse shear effects in their well-known First Order Shear Deformation Theory (FSDT). More accurate theories such as higher order theories (HOT) assume quadratic, cubic, higher variations or non-polynomial terms to improve the displacement field along the thickness direction [7-14].

However, the abovementioned theories may be not sufficient if local effects are important or accuracy in the calculation of the transverse stresses is required. The Zig-Zag models [15, 16] and mixed variational tools [17] have been proposed to deal with these phenomena. Among the plate models for laminated structures two different approach can be distinguished: the Equivalent Single Layer (ESL) and the Layer-Wise (LW) models. Excellent reviews of existing ESL and LW models can be found in [18-22].

This paper makes use of trigonometric and exponential expansions to build refined plate models. Shimpi and Ghugal [12], proposed a LW trigonometric shear deformation theory for the analysis of composite beams. Arya et al. [13] developed a Zig-Zag model using a sine term to represent the non-linear displacement field across the thickness in symmetric laminated beams. Ferreira et al. [14] presented a LW plate model using a meshless discretization method for symmetric composite plates. Mantari et al. [23] developed a new ESL plate model in which a parameter m was included on the trigonometric functions to obtain 3D like elasticity solutions. Mantari et al. [24] extended [23] to a LW plate model for finite element analysis of sandwich and composite laminated plate. Thai et al. [25, 26] presented isogeometric finite element formulations for static, free vibration and buckling analysis of laminated composite and sandwich plates. This was extended to a generalized shear deformation theory by Thai et al. [27]. Hybrid Maclaurin-trigonometric models were proposed by Mantari et al. [28, 29] for bending,

free vibration and buckling analysis of laminated beams. Mantari et al. [30] presented a generalized hybrid formulation for the study of functionally graded sandwich beams, which was extended to the Finite Element Method (FEM) by Yarasca et al. [31]. A unified framework on higher order shear deformation theories of laminated composite plates was proposed by Nguyen et al. [32]. Ramos et al. [33] developed refined theories based on non-polynomial kinematics via the Carrera Unified Formulation to deal with thermal problems, which was extended by Mantari et al. [34] to investigate the static behavior of FGM.

The refined models employed in this paper are based on the Carrera Unified Formulation (CUF). According to CUF, the governing equations are given regarding the so-called fundamental nuclei whose form does not depend on either the expansion order nor on the choices made for the base functions. This important feature allows to analyze any number of kinematic models in a single formulation and software. ESL and LW models were successfully developed in CUF, as reported in [35]. More details on CUF can be found in [36, 37]. To developed accurate refined theories with lower computational effort, Carrera and Petrolo [38, 39] introduced the Axiomatic/Asymptotic Method (AAM). This method consists of discarding all terms that do not contribute to the plate response analysis once a reference solution is defined. This leads to the development of reduced models whose accuracies are equivalent to those of full higher-order models. The AAM has been applied to several problems, including: static and free vibration of beams [38, 40], metallic and composite plates [39, 41], shells [42, 43], LW models [44, 45], advanced models based on the Reissner Mixed Variational Theorem [46], and piezoelectric plates [47].

The AAM method was adopted to build the BTD by Carrera et al. [48]. The BTD is a curve in which the minimum number of expansion terms - i.e. unknown variables -

required to meet a given accuracy can be read; or, conversely, the best accuracy provided by a given amount of variables can be read. To construct BTDs with a lower computational cost, a genetic algorithm was employed by Carrera and Miglioretti [49]. Petrolo et al. [50] presented BTDs for ESL and LW composite plate models based on Maclaurin and Legendre polynomial expansions of the unknown variables along the thickness.

The present work presents BTDs using Maclaurin, trigonometric and exponential thickness expansions for the analysis of laminated composite plates. The functions employed in this paper were selected according to Filippi et al. [51, 52]. Genetic algorithms are employed to reduce the computational cost related to the definition of the BTD.

The present paper is organized as follows: a description of the adopted formulation is provided in Section 2; the governing equations and closed-form solution is presented in Section 3; the AAM is presented in Section 4; the BTD is introduced in Section 5; the results are presented in Section 6, and the conclusions are drawn in Section 7.

2.   Carrera Unified Formulation for Plates

The geometry and the coordinate system of the multilayered plate of L layers are shown in Fig. 1. The integer k denotes the layer number that starts from the plate-bottom, x and y are the in-plane coordinates while z is the thickness coordinate.

In the framework of CUF, the displacement of a plate model can be described as:

$$\boldsymbol{u}(x, y, z) = F_\tau(z) \cdot \boldsymbol{u}_\tau(x, y) \qquad \tau = 1, 2, \dots, N + 1 \tag{1}$$

where $\boldsymbol{u}$ is the displacement vector (u_x, u_y, u_z) whose components are the displacements along the x, y and z reference axes. F_τ are the expansion functions and $\boldsymbol{u}_\tau$ $(u_{x_\tau}, u_{y_\tau}, u_{z_\tau})$ are the displacements variables. If an ESL scheme is employed, the behavior of a multilayered plate is analyzed considering it as a single equivalent lamina. In this case, F_τ functions can be Maclaurin functions of z defined as $F_\tau = z^{\tau-1}$. The ESL models are indicated as EDN, where N is the expansion order. An example of an ED4 displacement field is reported as:

$$u_x = u_{x_1} + z\, u_{x_2} + z^2 u_{x_3} + z^3 u_{x_4} + z^4 u_{x_5}$$

$$u_y = u_{y_1} + z\, u_{y_2} + z^2 u_{y_3} + z^3 u_{y_4} + z^4 u_{y_5}$$

$$u_z = u_{z_1} + z\, u_{z_2} + z^2 u_{z_3} + z^3 u_{z_4} + z^4 u_{z_5} \tag{2}$$

The present paper investigates the influence of trigonometric and exponential terms in ESL theories for laminated composite plates. The complete ED17 set of terms adopted is reported in Table 1. The displacement field of ED17 consists of 51 unknown variables, which include 15 Maclaurin terms - the ED4 terms -, 24 trigonometric terms and 12 exponential terms. For instance, the full expression of the displacement along x is

$$u_x = u_{x_1} + z\, u_{x_2} + z^2 u_{x_3} + z^3 u_{x_4} + z^4 u_{x_5} + \sin\left(\frac{\pi z}{h}\right) u_{x_6} + \sin\left(\frac{2\pi z}{h}\right) u_{x_7}$$

$$+ \sin\left(\frac{3\pi z}{h}\right) u_{x_8} + \sin\left(\frac{4\pi z}{h}\right) u_{x_9} + \cos\left(\frac{\pi z}{h}\right) u_{x_{10}} + \cos\left(\frac{2\pi z}{h}\right) u_{x_{11}} +$$

$$+ \cos\left(\frac{4\pi z}{h}\right) u_{x_{13}} + e^{\frac{z}{h}} u_{x_{14}} + e^{\frac{2z}{h}} u_{x_{15}} + e^{\frac{3z}{h}} u_{x_{16}} + e^{\frac{4z}{h}} u_{x_{17}} \tag{3}$$

where h is the thickness of the plate.

6

3. Governing equations and Closed-form solution

Geometrical relations enable to express the in-plane ϵ_p^k and the out-planes ϵ_n^k strains in terms of the displacement $\boldsymbol{u}$.

$$\epsilon_p^k = \left[\epsilon_{xx}^k,\ \epsilon_{yy}^k,\ \epsilon_{xy}^k\right]^T = \left(\boldsymbol{D}_p^k\right)\boldsymbol{u}^k, \quad \epsilon_n^k = \left[\epsilon_{xz}^k,\ \epsilon_{yz}^k,\ \epsilon_{zz}^k\right]^T = \left(\boldsymbol{D}_{np}^k + \boldsymbol{D}_{nz}^k\right)\boldsymbol{u}^k \quad (4)$$

where $\boldsymbol{D}_p^k, \boldsymbol{D}_{np}^k$ and $\boldsymbol{D}_{nz}^k$ are differential operators whose components are:

$$\boldsymbol{D}_p^k = \begin{bmatrix} \frac{\partial}{\partial x} & 0 & 0 \\ 0 & \frac{\partial}{\partial y} & 0 \\ \frac{\partial}{\partial y} & \frac{\partial}{\partial x} & 0 \end{bmatrix}, \quad \boldsymbol{D}_{np}^k = \begin{bmatrix} 0 & 0 & \frac{\partial}{\partial x} \\ 0 & 0 & \frac{\partial}{\partial y} \\ 0 & 0 & 0 \end{bmatrix}, \quad \boldsymbol{D}_{nz}^k = \begin{bmatrix} \frac{\partial}{\partial z} & 0 & 0 \\ 0 & \frac{\partial}{\partial z} & 0 \\ 0 & 0 & \frac{\partial}{\partial z} \end{bmatrix} \quad (5)$$

Stress components for a generic k layer can be obtained using the Hooke law,

$$\sigma_p^k = \boldsymbol{C}_{pp}^k \epsilon_p^k + \boldsymbol{C}_{pn}^k \epsilon_n^k$$

$$\sigma_n^k = \boldsymbol{C}_{np}^k \epsilon_p^k + \boldsymbol{C}_{nn}^k \epsilon_n^k \quad (6)$$

where matrices $\boldsymbol{C}_{pp}^k, \boldsymbol{C}_{pn}^k, \boldsymbol{C}_{np}^k$ and $\boldsymbol{C}_{nn}^k$ are:

$$\boldsymbol{C}_{pp}^k = \begin{bmatrix} C_{11}^k & C_{12}^k & C_{16}^k \\ C_{12}^k & C_{22}^k & C_{26}^k \\ C_{16}^k & C_{26}^k & C_{66}^k \end{bmatrix}, \qquad \boldsymbol{C}_{pn}^k = \begin{bmatrix} 0 & 0 & C_{13}^k \\ 0 & 0 & C_{23}^k \\ 0 & 0 & C_{36}^k \end{bmatrix},$$

$$\boldsymbol{C}_{np}^k = \begin{bmatrix} 0 & 0 & 0 \\ 0 & 0 & 0 \\ C_{13}^k & C_{23}^k & C_{36}^k \end{bmatrix}, \qquad \boldsymbol{C}_{nn}^k = \begin{bmatrix} C_{55}^k & C_{45}^k & 0 \\ C_{45}^k & C_{44}^k & 0 \\ 0 & 0 & C_{33}^k \end{bmatrix}, \quad (7)$$

For the sake of brevity, the dependence of the elastic coefficients C_{ij}^k on Young's modulus, Poisson's ratio, the shear modulus, and the fiber angle is no reported. They can be found in [9].

The governing equations are obtained via the principle of virtual displacement (PVD), which states that:

$$\delta L_{int} = \delta L_{ext} \tag{8}$$

where δL_{int} is the virtual variation of the internal work and δL_{ext} is the virtual variation of the work made by the external loadings. The PVD can be written as:

$$\sum_{k=1}^{N_l} \int_V \left(\delta \boldsymbol{\epsilon}_p^k \boldsymbol{\sigma}_p^k + \delta \boldsymbol{\epsilon}_n^k \boldsymbol{\sigma}_n^k \right) dV = \sum_{k=1}^{N_l} \delta L_{ext}^k \tag{9}$$

Further details about the CUF and its implementation through the use of variational principles can be found in [37]. The governing equations are expressed in compact form,

$$\delta \boldsymbol{u}_s^k \colon \ \boldsymbol{K}_d^{k\tau s} \boldsymbol{u}_\tau^k = \boldsymbol{P}_s^k \tag{10}$$

where $\boldsymbol{P}_\tau^k$ is the external load. The fundamental nucleus , $\boldsymbol{K}_d^{k\tau s}$, is assembled through the indexes τ and s to obtain the stiffness matrix of each layer k. Then, the matrices of each layer are assembled at the multilayer level depending on the approach considered, for this work the ESL approach is adopted.

In this paper, the closed-form solution proposed by Navier for simply supported orthotropic plates is exploited. The following properties hold:

$$C_{pp16} = C_{pp26} = C_{pn36} = C_{nn45} = 0 \tag{11}$$

The displacements are expressed in the following harmonic form,

$$u_x = \sum_{m,n} U_x \cdot \cos\left(\frac{m\pi x}{a}\right) \sin\left(\frac{n\pi y}{b}\right)$$

$$u_y = \sum_{m,n} U_y \cdot \cos\left(\frac{m\pi x}{a}\right) \sin\left(\frac{n\pi y}{b}\right)$$

$$u_z = \sum_{m,n} U_z \cdot \cos\left(\frac{m\pi x}{a}\right) \sin\left(\frac{n\pi y}{b}\right) \tag{12}$$

where U_x, U_y and U_z are the amplitudes, m and n are the number of waves, and a and b are the dimensions of the plate in the x and y directions, respectively.

4. Axiomatic/Asymptotic Method

The introduction of high order terms in a plate model offers significant advantages in terms of improved structural response analysis at the expense of higher computational cost. The axiomatic/asymptotic method (AAM) allows us to decrease the computational cost of a model and at the same time preserve the accuracy of a high order model. The AAM procedure can be summarized as follows:

(1) Parameters such as geometry, boundary conditions, loadings, materials and layer layouts are fixed.

(2) A set of output parameters is chosen, such as displacement and stress components.

(3) A theory is fixed; that is the displacement variables to be analyzed are defined.

(4) A reference solution is defined; in the present work, fourth-order LW models (LD4) are adopted.

(5) The CUF is used to generate the governing equations for the considered theories.

(6) Each variable displacement effectiveness is numerically established measuring the loss of accuracy on the chosen output parameters compared with the reference solution.

(7) The most suitable kinematic model for a given structural problem is then obtained by discarding the noneffective displacement variables.

A graphical notation is introduced to represent the results. This consists of a table with three rows, and some columns equal to the number of the displacement variable used

in the expansion. As an example, an ED4 model (full model) and a reduced model in which the term u_{x_2} is deactivated is shown in Table 2. The meaning of the symbols ▲ and Δ is reported in Table 3. The displacement field of Table 2 is

$$u_x = u_{x_1} + \qquad z^2 u_{x_3} + z^3 u_{x_4} + z^4 u_{x_5}$$

$$u_y = u_{y_1} + z\, u_{y_2} + z^2 u_{y_3} + z^3 u_{y_4} + z^4 u_{y_5}$$

$$u_z = u_{z_1} + z\, u_{z_2} + z^2 u_{z_3} + z^3 u_{z_4} + z^4 u_{z_5} \tag{13}$$

5.   Best Theory Diagram

The construction of reduced models through the AAM allows one to obtain a diagram, which for a given problem, each reduced model is associated with the number of active terms and its error computed on a reference solution. This diagram allows editing an arbitrary given theory to get a lower number of terms for a given error, or to increase the accuracy while keeping the computational cost constant. Considering all the reduced models, it is possible to recognize that some of them provide the lowest error for a given number of terms. These models represent a Pareto front for this specific problem. As in [49], the Pareto front is defined as the best theory diagram (BTD). It should be noted that the diagram changes for different conditions, i.e. different materials, geometries, loadings, boundary conditions and output parameters.

The AAM is a practical technique that allows us to obtain the BTD for a given problem. However, if the plate model has a large number of terms, the computational cost required for the BTD construction can be considerable. The number of all possible combinations of active/not-active terms for a given model is equal to 2^M, where M is the number of unknown variables (DOF) in the model. In the case considered in this paper,

M is equal to 51. Since the AAM evaluates every reduced plate model in order to build the BTD, a different strategy is needed.

In genetic algorithms terminology, a solution vector $\boldsymbol{x} \in \boldsymbol{X}$, where $\boldsymbol{X}$ is the solution space, is called an *individual* or *chromosome*. Chromosomes are made of discrete units called *genes*. Each gene controls one or more features of the individual. GAs operate with a collection of chromosomes, called a *population*. The population is normally randomly initialized. As the search evolves, the population includes fitter and fitter solutions, and eventually it converges, meaning that it is dominated by a single solution. Simple GAs use three operators to generate new solutions from existing ones: *reproduction*, *crossover* and *mutation*. On the reproduction, individuals with higher fitness are preserve for the next generation. Each individual has a fitness value based on its rank in the population. The population is ranked according to a dominance rule. The fitness of each chromosome is evaluated throught the following formula:

$$r_i(\boldsymbol{x_i}, t) = 1 + nq(\boldsymbol{x_i}, t) \tag{14}$$

where $nq(\boldsymbol{x}, t)$ is the number of solutions dominating $\boldsymbol{x}$ at generation t. A lower rank corresponds to a better solution. On the crossover, generally two chromosomes, called *parents*, are combined together to form new chromosomes, called *offsprings*. The mutation operator introduces random changes at gene level. In this paper an elitism technique is used in order to preserve the dominant individuals in each generation without any changes in its configuration. A complete explanation on genetic algorithms can be found in [53,54].

Each plate theory has been considered as an individual. The genes are the terms of the expansion along the thickness of the three displacement fields in the following manner. Each gene can be active or not, the deactivation of a term is obtained by

exploiting a penalty or row-column elimination technique. The representation of this method is shown in Fig 2. Each individual is therefore described by the number of active terms and its error that is computed on a reference solution. The dominance rule is applied through these two parameters to evaluate the individual fitness. The error of the new models on a reference solution was evaluated through the following formula:

$$e = 100 \frac{\sum_{i=1}^{N_p} |Q^i - Q_{ref}^i|}{max Q_{ref} \cdot N_p} \tag{15}$$

where Q can be a stress/displacement component ($\bar{\sigma}_{xx}$ and $\bar{\tau}_{xz}$ in this article) and N_p is the number of points along the thickness on which the entity Q is computed. Each chromosome of the new population its ranked and new dominant chromosomes are selected. More details about the implementation of genetic algorithms for BTD can be found in [49]. In this paper, 50 generations were used and the initial population was set to 500.

6.   Results and discussion

A bisinusoidal load is applied to the top surface of the simply supported laminated plate:

$$p = \bar{p}_z \cdot sin\left(\frac{m\pi x}{a}\right) sin\left(\frac{n\pi y}{b}\right) \tag{16}$$

where $a = b = 0.1\ m$. $\bar{p}_z$ is the applied load amplitude, $\bar{p}_z = 1\ kPa$, and m and n are equal to 1. The reduced models are developed for σ_{xx} and τ_{xz}. The axial and shear stress are computed at $\left[a/2, b/2, z\right]$ and $\left[0, b/2, z\right]$, with $-\frac{h}{2} \leq z \leq \frac{h}{2}$. h is the total thickness of the plate. The stresses are normalized according to:

$$\bar{\sigma}_{xx} = \frac{\sigma_{xx}}{\bar{p}_z \cdot (a/h)^2}, \qquad \bar{\tau}_{xz} = \frac{\tau_{xz}}{\bar{p}_z \cdot (a/h)} \tag{17}$$

The material properties are: $E_L/E_T = 25$; $G_{LT}/E_T = 0.5$; $G_{TT}/E_T = 0.2$; $\nu_{LT} = \nu_{TT} = 0.25$. Each layer has the same thickness. Two length-to-thickness ratios are investigated: $a/h = 4$ and $a/h = 20$. The numerical investigation considered three reference problems:

- A three layer cross-ply square plate with lamination 0º/90º/0º.

- A two layer cross-ply square plate with lamination 0º/90º.

- A four layer cross-ply square plate with lamination 0º/90º/90º/0º.

To set a reference solution, an LD4 model assessment was carried out. The results are reported in Table 4; the three-dimensional exact elasticity results were taken from [55, 56]. The LD4 are in excellent agreement with the reference solution. Consequently, the LD4 model is used as the reference solution in this paper.

6.1   *Three layer cross-ply square plate 0º/90º/0º*

The first method that was used to build the BTD was based on the evaluation of all possible combinations of an ED4 polynomial model obtain by the AAM. Figure 3 shows the error of each theory and the corresponding BTD built by the AAM. A genetic algorithm is used to build the reduced ED17 plate models with low computational cost. To corroborate the convergence of the GA to the Pareto front, a comparison between the BTDs obtained by the GA and the AAM is presented in Figure 3. It is clear that the BTDs obtained are in complete agreement. Figures 4a and 4b show the difference between the BTDs built from a polynomial ED4 model and the reduce ED17 model with trigonometric and exponential terms for length-to-thickness ratios equal to 4 and 20. The error is calculated according to Eq. (15), where Q is the stress $\bar{\sigma}_{xx}$. The notation used is the following: the BTD built from a polynomial ED4 model is indicated as *Pol*; the BTD

built from the ED17 model is referred to as *Hybrid*. For the sake of clarity, only plate

theories with 15 terms or less are reported to allow a straightforward comparison with the

ED4 model. Some of the BTD models are given Fig. 4a and Fig. 4b are reported in Tables

5 and 6, respectively. The number of active terms is indicated by M_E. For instance, the

best hybrid model for $\bar{\sigma}_{xx}$ with six unknown variables corresponds to the following

displacement field:

$$u_x = z^3 u_{x_4} + \sin\left(\frac{\pi z}{h}\right) u_{x_6} + \sin\left(\frac{3\pi z}{h}\right) u_{x_8}$$

$$u_y = z u_{y_2}$$

$$u_z = u_{z_1} + e^{\frac{4z}{h}} u_{z_{17}} \tag{18}$$

Similarly, the best plate model for $\bar{\sigma}_{xx}$ obtained via ED4 with six unknown

variables is

$$u_x = z u_{x_2} + z^3 u_{x_4}$$

$$u_y = z u_{y_2} + z^3 u_{y_4}$$

$$u_z = u_{z_1} + z u_{z_2} \tag{19}$$

For comparison purposes, the errors of the reduced plate models obtained via ED4

and those from hybrid models are presented in Table 7. The results clearly show that the

addition of non-polynomial terms can improve considerably the performance of higher-

order plate theories. For example, the plate model of Eq. (18) can detect $\bar{\sigma}_{xx}$ with 1.4720

% of error, while the plate model of Eq. (19) has an error of 4.1897 %. In Fig. 5, the

distribution through the thickness of $\bar{\sigma}_{xx}$ is shown for different plate length-to-thickness

ratios. The evaluation of $\bar{\sigma}_{xx}$ is performed by means of the reduced models reported in

Tables 5 and 6. The notation used is N HRM, where N is the number of variables in the hybrid reduced models (HRM). The reference solution (LD4) and the best reduced N ED4 plate model is included for comparison purposes.

Figures 6a and 6b show the BTDs obtained for $\bar{\tau}_{xz}$ with $a/h = 4$ and $a/h = 20$, respectively. $\bar{\tau}_{xz}$ was obtained via 3D equilibrium equations. Hybrid plate models from the BTDs in Fig. 6 are reported in Tables 8 and 9, and a comparison between the hybrid models considered and plate models obtained from ED4 is reported in Table 10. In Fig. 7, $\bar{\tau}_{xz}$ distribution along the thickness for the length-to-thickness ratio mentioned is presented.

The results herein reported for the symmetric cross-ply square plate 0º/90º/0º suggest that:

- The GA approach is a reliable and computationally inexpensive tool to build BTDs.

- The addition of trigonometric and exponential expansion terms can improve the effeciency of plate models. In particular, such terms can lead to higher accuracies than purely Macluarin-based models.

- In general, the trigonometric terms are more effective than the exponential ones.

- In all cases, the reduced best models can detect the 3D-like, LW solution with a considerable lower amount of unknown variables. Some ten generalized displacement variables are usually enough to meet satisfactory accuracy levels.

6.2   Two layer cross-ply square plate 0º/90º

BTDs for $\bar{\sigma}_{xx}$ are presented in Fig. 8. Selected BTD models for both length-to-thickness ratios are reported in Tables 11 and 12, repectively. For example, the best hybrid model with seven degrees of freedom for the stress $\bar{\sigma}_{xx}$ and $a/h = 4$ is the following:

$$u_x = u_{x_1} + z u_{x_2} + \sin\left(\frac{2\pi z}{h}\right) u_{x_7}$$

$$u_y = u_{y_1} + z u_{y_2}$$

$$u_z = u_{z_1} + e^{\frac{z}{h}} u_{z_{14}} \tag{20}$$

Likewise, the best Maclaurin model for $\bar{\sigma}_{xx}$ for the same case is:

$$u_x = u_{x_1} + z u_{x_2} + z^2 u_{x_3} + z^4 u_{x_5}$$

$$u_y = u_{y_1} + z u_{y_2}$$

$$u_z = u_{z_1} \tag{21}$$

The same theories considered are compared with the reduced ED4 plate models in Table 13. Figure 9 shows the stress distribution along the thickness. BTDs for $\bar{\tau}_{xz}$ are presented in Fig. 10, whereas Fig. 11 shows the shear stress distribution along the thickness.

The results reported for the asymmetric cross-ply square plate 0º/90º suggest that:

- Concerning $\bar{\sigma}_{xx}$, significant improvements were observed on the BTD by including non-polynomial terms, especially fot the thick plate case. In particular, trigonometric and exponential terms have a similar relevance.
- Concerning $\bar{\tau}_{xz}$, both ED4 and ED17 reduced models are in agreement with the LD4 results. In other words, the inclusion of exponential and trigonometric terms is less relevant than in the previous cases.

6.3   *Four layer cross-ply square plate 0º/90º/90º/0º*

The BTDs for $\bar{\sigma}_{xx}$ is shown in Fig. 12 via the ED4 and ED17 expansions, for $^a/_h = 4$ and

$a/_h$ = 20. Some plate theories belonging to the BTD are presented in Tables 14 and 15. Table 16 presents the accuracy of the models, whereas the stress distribution along the thickness is given in Fig. 13. BTDs for $\bar{\tau}_{xz}$ are presented in Fig. 14. In Tables 17 and 18, BTD plate theories are reported for $a/_h = 4$ and $a/_h = 20$, respectively. The shear stress distribution along the thickness is shown in Fig. 15. For instance, the best hybrid model with six degrees of freedom for the stress $\bar{\tau}_{xz}$ and $a/_h = 4$ is the following:

$$u_x = zu_{x_2} + z^3u_{x_4} + \sin\left(\frac{\pi z}{h}\right)u_{x_6} + e^{\frac{3z}{h}}u_{x_{16}}$$

$$u_y = zu_{y_2}$$

$$u_z = u_{z_1} \tag{22}$$

Likewise, the best Maclaurin model for the same case is:

$$u_x = u_{x_1} + zu_{x_2} + z^3u_4$$

$$u_y = zu_{y_2}$$

$$u_z = u_{z_1} + zu_{z_2} \tag{23}$$

The results reported for the 0°/90°/90°/0° plate suggest that:

- For $\bar{\sigma}_{xx}$ and $\bar{\tau}_{xz}$, a 3D like accuracy is obtained by employing non-polynomial terms in the plate models. This is particulary significant for thick plates were the improvements achieved are noteworthy.

- As seen in the previous cases, the adoption of exponential and trigonometric terms is useful to improve the accuracy of the model, and their influence is more

relevant for thick plates. In particular, the exponential terms are more effective than the tringonometric terms for the laminated composite plate studied.

7.   Conclusion

Best Theory Diagrams (BTDs) for cross-ply laminated plates have been presented in this paper. The BTD is a curve in which, for a given probelem, the most accurate plate models for a given number of unknown variables can be read. The axiomatic/asymptotic method and genetic algorithms have been employed together with the Carrera Unified Formulation to develop refined ESL models. In particular, a combination of Maclaurin, trigonometric and exponential polynomials has been used to define the displacement field along the thickness of the plate. The results have been presented in terms of the in-plane stress $\bar{\sigma}_{xx}$ and the shear stress $\bar{\tau}_{xz}$ for different length-to-thickness ratios. Simply-supported plates have been analyzed via Navier-type closed form solutions. The present paper has highlighted the importance of non-polynomial terms on plate models. In particular:

(1) The use of the AAM and the BTD leads to enhanced refined models yielding quasi-3D results with small computational costs.

(2) For thick plates, the use of non-polynomial terms is of fundamental to obtain 3D-like accuracies.

(3) For moderately thick plates, the importance of exponential and trigonometric terms is smaller.

(4) The importance of exponential and trigonometric terms vary depending on the plate configuration. For plates with lamination 0º/90º/0º, trigonometric terms are more important than exponential ones.

(5) For plates with lamination 0º/90º, exponential and trigonometric terms have similar relevance.

(6) For plates with lamination 0º/90º/90º/0º, exponential terms are more effective than the trigonometric ones.

The combined use of CUF, AAM and genetic algorithms allows us to obtain BTDs with low computational efforts. The BTD can be seen as a tool to evaluate the effectiveness of any structural model. In fact, any type and order of expansions of the unknown variables can be dealt with in a unified manner. Future works should tackle the construction of BTDs for multiple outputs (stresses and displacements) and dynamic problems.

References

[1] Cauchy AL. Sure l'equilibre et le movement d'une plaque solide. Excercies Matematique 1828;3:328-55.

[2] Poisson SD. Memoire sur l'equilibre et le mouvement des corps elastique. Mem l'Acad Sci 1829;8:357.

[3] Kirchhoff G. Über das Gleichgewicht und die Bewegung einer elastishen Scheibe. J Angew Math 1850; 40: 51-88.

[4] Love AEH The Mathematical Theory of Elasticity, 4th Edition, Cambridge Univ Press, Cambridge, 1927

[5] Reissner E. The effect of transverse shear deformation on the bending of elastic plates. J Appl Mech 1945; 12:69-76.

[6] Mindlin RD. Influence of rotatory inertia and shear in flexural motion of isotropic elastic plates. J Appl Mech 1951; 18: 1031-6.

[7] Kant T, Owen DRJ, Zienkiewicz OC. Refined higher order C0 plate bending element. Comput Struct 1982;15:177–83.

[9] Reddy JN. Mechanics of Laminated Plates, Theory and Analysis. CRC Press, Boca Raton, FL, 1997.

[10] Palazotto AN, Dennis ST. Nonlinear analysis of shell structures. AIAA Series; 1992.

[11] M. Touratier. An efficient standard plate theory. International Journal of Engineering Science 1991, 29(8):901 – 916.

[12] Shimpi RP, Ghugal YM. A new layerwise trigonometric shear deformation theory for two-layered cross-ply beams. Compos Sci Technol 2001;61 (9):1271–83.

[13] Arya H, Shimpi RP, Naik NK. A zigzag model for laminated composite beams. Compos Struct 2002;56(1):21–4.

[14] Ferreira AJM, Roque CMC, Jorge RMN. Analysis of composite plates by trigonometric shear deformation theory and multiquadrics. Comp. and Struct. 2005;83(27):2225–37.

[15] G.S. Lekhnitskii, Anisotropic Plates, 2nd Edition, SW Tsai and Cheron, Bordon and Breach, Cooper Station, NY, 1968.

[16] E. Carrera, Historical review of zig-zag theories for multilayered plates and shells, Appl. Mech. Rev. 2003, vol. 56, no. 3, pp. 287–308.

[17] E. Reissner, On a mixed variational theorem and on a shear deformable plate theory, Int. J.Numer.Methods Eng. 1986, vol. 23, pp. 193–198.

[18] Librescu L, Reddy JN. A critical review and generalization of transverse shear deformable anisotropic plates. In: Euromech Colloquium 219, Kassel, Refined Dynamical Theories of Beams, Plates and Shells and Their Application, I. Elishakoff and H. Irretier, Ess., Springer-Verlag, Berlin, 1986.

[19] Noor AK, and Burton WS. Assessments of Shear Deformation Theories for Multilayered Composite Plates. Applied Mechanics Reviews. 42, 1989, pp. 1-18.

[20] Noor AK, Burton WS and Bert CW. Computational Model for Sandwich Panels and Shells. Applied Mechanics Reviews. 49, 1996, pp. 155-199.

[21] Kapania K, Raciti S. Recent advances in analysis of laminated beams and plates. Part 1: Shear effects and buckling. AIAA J 1989; 27(7); 923-35.

[22] Reddy JN, Robbins DH. Theories and Computational Models for Composite Laminates. Applied Mechanics Reviews. 47, 1994, pp. 147-165.

[23] Mantari JL, Oktem AS, Guedes Soares C. A new trigonometric shear deformation theory for isotropic, laminated composite and sandwich plates. Int. J. of Sol. and Struct. 2012; 49; pp. 43-53.

[24] Mantari JL, Oktem AS, Guedes Soares C. A new trigonometric layerwise shear deformation theory for the finite element analysis of laminated composite and sandwich plates. Comp. and Struct. 2012; 94-95; pp. 45-53.

[25] Thai CH, Ferreira AJM, Carrera E, Nguyen-Xuan H. Isogeometric analysis of laminated composite and sandwich plates using a layerwise deformation theory. Comp. and Struct. 2013; 104; pp. 196-214.

[26] Nguyen-Xuan H, Thai CH, Nguyen-Thoi. Isogeometric finite element analysis of composite sandwich plates using a higher order shear deformation theory. Comp. Part B. 2013; 55; pp. 558-574.

[27] Thai CH, Kulasegaram S, Tran LV, Nguyen-Xuan H. Generalized shear deformation theory for functionally graded isotropic and sandwich plates based on isogeometric approach. Comp. and Struct. 2014; 141; pp. 94-112.

[28] Mantari JL, Canales FG. A unified quasi-3D HSDT for the bending analysis of laminated beams. Aerospace Science and Technology 2016; 54, pp. 267-275.

[29] Mantari JL, Canales FG. Free vibration and buckling of laminated beams via hybrid Ritz solution for various penalized boundary conditions. Composite Structures 2016; http://dx.doi.org/10.1016/j.compstruct.2016.05.037.

[30] Mantari JL, Yarasca J. A simple and accurate generalized shear deformation theory for beams. Composite Structures 2015; 134, pp. 593-601.

[31] Yarasca J, Mantari JL, Arciniega RA. Hermite–Lagrangian finite element formulation to study functionally graded sandwich beams. Composite Structures 2016; 140, pp 567-581.

[32] Nguyen TN, Thai CH, Nguyen-Xuan H. On the general framework of high order shear deformation theories for laminated composite plate structures: A novel unified approach. Int. J. of Mech. Sci. 2016; 110; pp. 242-255.

[33] Ramos IA, Mantari JL, Pagani A, Carrera E. Refined theories based on non-polynomial kinematics for the thermoelastic analysis of functionally graded plates, Journal of Thermal Stresses 2016; 39(7):835-853.

[34] Mantari JL, Ramos IA, Carrera E, Petrolo M. Static analysis of functionally graded plates using new non-polynomial displacement fields via Carrera Unified Formulation, Composites Part B 2016; 89:127-142.

[35] Carrera E. Theories and finite elements for multilayered plates and shells: a unified compact formulation with numerical assessment and benchmarking. Arch Comput Meth Eng 2003; 10(3): 215-96.

[36] Carrera E, Brischetto S, Nali P. Plates and shells for smart structures classical and advanced theories for modeling and analysis. Wiley; 2011.

[37] Carrera E, Cinefra M, Petrolo M, Zappino E. Finite Element Analysis of Structures through Unified Formulation. John Wiley & Sons, Inc., Chichester, UK, 2014.

[38] Carrera E, Petrolo M. On the effectiveness of higher-order terms in refined beam theories. Journal of Applied Mechanics 2011; 78. doi: 10.1115/1.4002207.

[39] Carrera E, Petrolo M. Guidelines and recommendation to construct theories for metallic and composite plates. AIAA J. 2012; 48(12): 2852-2866.

[40] Carrera E, Miglioretti F, Petrolo M. Computations and evaluations of higher-order theories for free vibration analysis of beams. Journal of Sound and Vibration 2012; 331:4269-4284. doi: 10.1016/j.jsv.2012.04.017.

[41] Mashat DS, Carrera E, Zenkour AM, Khateeb Al. Axiomatic/asymptotic evaluation of multilayered plate theories by using single and multi-points error criteria. Compos Struct 2013; 106, pp. 393-406.

[42] Mashat DS, Carrera E, Zenkour AM, Khateeb Al. Use of axiomatic/asymptotic approach to evaluate various refined theories for sandwich shells. Compos Struct 2013; 109, pp. 139-149.

[43] Mashat DS, Carrera E, Zenkour AM, Al Katheeb SA, Lamberti A. Evaluation of refined theories for multilayered shells via Axiomatic/Asymptotic method. Journal of Mechanical Science and Technology 2014; 28(11):4663-4672.

[44] Carrera E, Cinefra M, Lamberti A, Petrolo M. Results on best theories for metallic and laminated shells including Layer-Wise models. Composite Structures 2015; 126:285-298.

[45] Petrolo M, Lamberti A. Axiomatic/asymptotic analysis of refined layer-wise theories for composite and sandwich plates. Mech Adv Mater Struct 2016; 23(1): 28-42.

[46] Petrolo M, Cinefra M, Lamberti A, Carrera E. Evaluation of Mixed Theories for Laminated Plates through the Axiomatic/Asymptotic Method. Composites Part B 2015; 76:260-272.

[47] Cinefra M, Lamberti A, Zenkour Ashraf M, Carrera E. Axiomatic/Asymptotic Technique Applied to Refined Theories for Piezoelectric Plates. Mechanics of Advanced Materials and Structures 2015; 22(1-2):107-124.

[48] Carrera E, Miglioretti F, Petrolo M. Guidelines and recommendations on the use of higher order finite elements for bending analysis of plates, Int J Comput Methods Eng Sci Mech 2011; 12(6), pp. 303-324.

[49] Carrera E, Miglioretti F. Selection of appropriate multilayered plate theories by using a genetic like algorithm. Composite Structures 2012; 94(3):1175-1186. doi: 10.1016/j.compstruct.2011.10.013.

[50] Petrolo M, Lamberti A, Miglioretti F. Best theory diagram for metallic and laminated composie plates. Mech Adv Mater Struct 2016; 23:9, pp. 1114-1130.

[51] Filippi M, Carrera E, Zenkour AM. Static analyses of FGM beams by various theories and finite elements. Composites Part B: Engineering 2015; 72, pp. 1-9.

[52] Filippi M, Petrolo M, Valvano S, Carrera E. Analysis of laminated composites and sandwich structures by trigonometric, exponential and miscellaneous polynomials and a MITC9 plate element. Composite Structures 2016; 150, pp. 103-114.

[53] Abdullah Konak, David W Coit, Alice E Smith. Multi-objective optimization using genetic algorithms: A tutorial. Reliability Engineering & System Safety 2006; 91 (9), pp. 992-1007.

[54] Deb K. Multi-Objective Optimization using Evolutionary Algorithms. John Wiley & Sons, Inc., Chichester, UK, 2001.

[55] Pagano JN, Exact solutions for rectangular bidirectional composites and sandwich plate, J. Compos. Mater., vol. 4, pp. 20–34, 1969.

[56] Pagano JN, Elastic behaviour of multilayered bidirectional composites, AIAA J., vol. 10, no. 7, pp. 931–933, 1972.

Tables

Table 1: Expansion terms of the proposed theories.

1	2	3	4	5	6	7	8	9
1	z	z^2	z^3	z^4	$\sin\left(\dfrac{\pi z}{h}\right)$	$\sin\left(\dfrac{2\pi z}{h}\right)$	$\sin\left(\dfrac{3\pi z}{h}\right)$	$\sin\left(\dfrac{4\pi z}{h}\right)$
1	z	z^2	z^3	z^4	$\sin\left(\dfrac{\pi z}{h}\right)$	$\sin\left(\dfrac{2\pi z}{h}\right)$	$\sin\left(\dfrac{3\pi z}{h}\right)$	$\sin\left(\dfrac{4\pi z}{h}\right)$
1	z	z^2	z^3	z^4	$\sin\left(\dfrac{\pi z}{h}\right)$	$\sin\left(\dfrac{2\pi z}{h}\right)$	$\sin\left(\dfrac{3\pi z}{h}\right)$	$\sin\left(\dfrac{4\pi z}{h}\right)$

10	11	12	13	14	15	16	17
$\cos\left(\dfrac{\pi z}{h}\right)$	$\cos\left(\dfrac{2\pi z}{h}\right)$	$\cos\left(\dfrac{3\pi z}{h}\right)$	$\cos\left(\dfrac{4\pi z}{h}\right)$	$e^{\frac{z}{h}}$	$e^{\frac{2z}{h}}$	$e^{\frac{3z}{h}}$	$e^{\frac{4z}{h}}$
$\cos\left(\dfrac{\pi z}{h}\right)$	$\cos\left(\dfrac{2\pi z}{h}\right)$	$\cos\left(\dfrac{3\pi z}{h}\right)$	$\cos\left(\dfrac{4\pi z}{h}\right)$	$e^{\frac{z}{h}}$	$e^{\frac{2z}{h}}$	$e^{\frac{3z}{h}}$	$e^{\frac{4z}{h}}$
$\cos\left(\dfrac{\pi z}{h}\right)$	$\cos\left(\dfrac{2\pi z}{h}\right)$	$\cos\left(\dfrac{3\pi z}{h}\right)$	$\cos\left(\dfrac{4\pi z}{h}\right)$	$e^{\frac{z}{h}}$	$e^{\frac{2z}{h}}$	$e^{\frac{3z}{h}}$	$e^{\frac{4z}{h}}$

Table 2: Example of model representation.

Full model representation					Reduced model representation				
▲	▲	▲	▲	▲	▲	Δ	▲	▲	▲
▲	▲	▲	▲	▲	▲	▲	▲	▲	▲
▲	▲	▲	▲	▲	▲	▲	▲	▲	▲

Table 3: Symbols to indicate the status of a displacement variable.

Active term	Inactive terms
▲	Δ

Table 4: LD4 model assessment for 3-layer and 5-layer laminated plates, $\bar{\sigma}_{xx/yy/xy} = \dfrac{\sigma_{xx}}{\bar{p}_z \cdot (a/h)^2}$, $\bar{\tau}_{xz/yz} = \dfrac{\tau_{xz}}{\bar{p}_z \cdot (a/h)}$.

	$a/h = 100$				
	3-layer laminate (0º/90º/0º)				
	$\bar{\sigma}_{xx}(z = \pm h/2)$	$\bar{\sigma}_{yy}(z = \pm h/6)$	$\bar{\tau}_{xz}(z = 0)$	$\bar{\tau}_{yz}(z = 0)$	$\bar{\tau}_{xy}(z = \pm h/2)$
Ref. [55]	±0.539	±0.181	0.395	0.0828	±0.0213
LD4	±0.539	±0.1808	0.3946	0.0828	±0.0213
	5-layer laminate (0º/90º/0º/90º/0º)				
	$\bar{\sigma}_{xx}(z = \pm h/2)$	$\bar{\sigma}_{yy}(z = \pm h/3)$	$\bar{\tau}_{xz}(z = 0)$	$\bar{\tau}_{yz}(z = 0)$	$\bar{\tau}_{xy}(z = \pm h/2)$
Ref. [56]	±0.539	±0.360	0.272	0.205	±0.0213
LD4	±0.5386	±0.3600	0.2720	0.2055	±0.0213

	$a/h = 4$						
	3-layer laminate (0º/90º/0º)						
	$\bar{\sigma}_{xx}(z = \pm h/2)$		$\bar{\sigma}_{yy}(z = \pm h/6)$		$\bar{\tau}_{xz}(z = 0)$	$\bar{\tau}_{yz}(z = 0)$	$\bar{\tau}_{xy}(z = \pm h/2)$
Ref. [55]	0.801	-0.755	0.534	-0.556	0.256	0.2172	-0.0511 0.0505
LD4	0.8008	-0.7547	0.5341	-0.5562	0.2559	0.2179	-0.0510 0.0505
	5-layer laminate (0º/90º/0º/90º/0º)						
	$\bar{\sigma}_{xx}(z = \pm h/2)$		$\bar{\sigma}_{yy}(z = \pm h/3)$		$\bar{\tau}_{xz}(z = 0)$	$\bar{\tau}_{yz}(z = 0)$	$\bar{\tau}_{xy}(z = \pm h/2)$
Ref. [56]	0.685	-0.651	0.633	-0.626	0.238	0.229	-0.0394 0.0384
LD4	0.6852	-0.6512	0.6334	-0.6256	0.2378	0.2289	-0.0393 0.0384

Table 5: Reduced ED17 models for stress $\bar{\sigma}_{xx}$, symmetric cross-ply laminated plate (0°/90°/0°), $a/h = 4$.

$$M_E = {}^{4}/_{51}$$

△	△	△	▲	△	▲	△	△	△	△	△	△	△	△	△	△	△
△	▲	△	△	△	△	△	△	△	△	△	△	△	△	△	△	△
▲	△	△	△	△	△	△	△	△	△	△	△	△	△	△	△	△

$$M_E = {}^{6}/_{51}$$

△	△	△	▲	△	▲	△	▲	△	△	△	△	△	△	△	△	△
△	▲	△	△	△	△	△	△	△	△	△	△	△	△	△	△	△
▲	△	△	△	△	△	△	△	△	△	△	△	△	△	△	△	▲

$$M_E = {}^{8}/_{51}$$

▲	△	△	▲	△	▲	△	▲	▲	△	△	△	△	△	△	△	△
△	▲	△	△	△	△	△	△	△	△	△	△	△	△	△	△	△
▲	△	△	△	△	△	△	△	△	△	△	△	△	▲	△	△	△

$$M_E = {}^{10}/_{51}$$

▲	△	▲	▲	△	▲	△	▲	▲	△	△	△	△	△	△	△	△
△	▲	△	△	△	△	△	△	△	△	△	△	△	△	△	△	△
▲	▲	△	△	△	△	△	△	△	△	△	△	△	▲	△	△	△

$$M_E = {}^{15}/_{51}$$

▲	▲	▲	▲	△	▲	△	▲	▲	▲	△	△	△	▲	▲	△	△
△	▲	△	▲	△	△	△	△	△	△	△	△	△	△	△	△	△
▲	▲	△	△	△	△	△	△	△	△	△	△	△	▲	△	△

Table 6: Reduced ED17 models for stress $\bar{\sigma}_{xx}$, symmetric cross-ply laminated plate (0°/90°/0°), $a/h = 20$.

$$M_E = {}^{5}/_{51}$$

△	▲	△	△	△	▲	△	▲	△	△	△	△	△	△	△	△	△
△	▲	△	△	△	△	△	△	△	△	△	△	△	△	△	△	△
▲	△	△	△	△	△	△	△	△	△	△	△	△	△	△	△	△

$$M_E = {}^{7}/_{51}$$

△	▲	△	▲	△	▲	△	▲	▲	△	△	△	△	△	△	△	△
△	▲	△	△	△	△	△	△	△	△	△	△	△	△	△	△	△
▲	△	△	△	△	△	△	△	△	△	△	△	△	△	△	△	△

$$M_E = {}^{9}/_{51}$$

△	▲	△	▲	△	▲	△	▲	▲	△	△	△	△	△	△	△	△
▲	▲	△	△	△	△	△	△	△	△	△	△	△	△	△	△	△
▲	△	▲	△	△	△	△	△	△	△	△	△	△	△	△	△	△

▲	▲	Δ	▲	Δ	▲	Δ	▲	▲	Δ	Δ	Δ	Δ	Δ	Δ	Δ	Δ
▲	▲	Δ	Δ	Δ	Δ	Δ	Δ	Δ	Δ	Δ	Δ	Δ	Δ	Δ	Δ	Δ
▲	Δ	▲	Δ	Δ	Δ	Δ	Δ	Δ	Δ	Δ	Δ	Δ	▲	Δ	Δ	Δ

Table 7: Comparison of the ED4 and ED17 reduced models for the $\bar{\sigma}_{xx}$ stress, symmetric cross-ply laminated plate (0°/90°/0°), $^a/_h = 4$ and $^a/_h = 20$.

$^a/_h = 4$			$^a/_h = 20$		
M_E	% Error – ED4	% Error – ED17	M_E	% Error – ED4	% Error – ED17
$^4/_{51}$	4.4664	2.5298	$^5/_{51}$	0.5847	0.3603
$^6/_{51}$	4.1897	1.4720	$^7/_{51}$	0.5814	0.0732
$^8/_{51}$	4.0691	1.1104	$^9/_{51}$	0.5814	0.0704
$^{10}/_{51}$	4.0685	0.7444	$^{11}/_{51}$	0.5814	0.0586
$^{15}/_{51}$	4.0685	0.5319			

Table 8: Reduced ED17 models for stress $\bar{\tau}_{xz}$ obtained via 3D equilibrium equations, symmetric cross-ply laminated plate (0°/90°/0°), $^a/_h = 4$.

$$M_E = {}^5/_{51}$$

Δ	▲	Δ	▲	Δ	▲	Δ	Δ	Δ	Δ	Δ	Δ	Δ	Δ	Δ	Δ	Δ
Δ	▲	Δ	Δ	Δ	Δ	Δ	Δ	Δ	Δ	Δ	Δ	Δ	Δ	Δ	Δ	Δ
▲	Δ	Δ	Δ	Δ	Δ	Δ	Δ	Δ	Δ	Δ	Δ	Δ	Δ	Δ	Δ	Δ

$$M_E = {}^8/_{51}$$

▲	Δ	Δ	▲	Δ	▲	Δ	▲	▲	Δ	Δ	Δ	Δ	Δ	Δ	Δ	Δ
Δ	▲	Δ	Δ	Δ	Δ	Δ	Δ	Δ	Δ	Δ	Δ	Δ	Δ	Δ	Δ	Δ
▲	Δ	Δ	Δ	Δ	Δ	Δ	Δ	Δ	Δ	Δ	Δ	Δ	Δ	Δ	Δ	▲

$$M_E = {}^{10}/_{51}$$

▲	Δ	▲	▲	Δ	▲	Δ	▲	▲	Δ	Δ	Δ	Δ	Δ	Δ	Δ	Δ
Δ	▲	Δ	Δ	Δ	Δ	Δ	Δ	Δ	Δ	Δ	Δ	Δ	Δ	Δ	Δ	▲
▲	▲	Δ	Δ	Δ	Δ	Δ	Δ	Δ	Δ	Δ	Δ	Δ	Δ	Δ	Δ	Δ

$$M_E = {}^{14}/_{51}$$

Δ	▲	▲	Δ	▲	▲	Δ	▲	▲	Δ	Δ	Δ	Δ	▲	▲	Δ	Δ
Δ	▲	Δ	Δ	Δ	▲	Δ	Δ	Δ	Δ	Δ	Δ	Δ	Δ	▲	Δ	Δ
▲	Δ	▲	Δ	Δ	Δ	Δ	Δ	Δ	Δ	Δ	Δ	▲	Δ	Δ	Δ	Δ

Table 9: Reduced ED17 models for stress $\bar{\tau}_{xz}$ obtained via 3D equilibrium equations, symmetric cross-ply laminated plate (0°/90°/0°), $a/h = 20$.

$$M_E = {}^5/_{51}$$

Δ	▲	Δ	▲	Δ	▲	Δ	Δ	Δ	Δ	Δ	Δ	Δ	Δ	Δ	Δ	Δ
Δ	▲	Δ	Δ	Δ	Δ	Δ	Δ	Δ	Δ	Δ	Δ	Δ	Δ	Δ	Δ	Δ
▲	Δ	Δ	Δ	Δ	Δ	Δ	Δ	Δ	Δ	Δ	Δ	Δ	Δ	Δ	Δ	Δ

$$M_E = {}^7/_{51}$$

Δ	▲	Δ	▲	Δ	▲	Δ	▲	Δ	Δ	Δ	Δ	Δ	Δ	Δ	Δ	Δ
Δ	▲	Δ	Δ	Δ	Δ	Δ	Δ	Δ	Δ	Δ	Δ	Δ	Δ	Δ	Δ	Δ
▲	Δ	▲	Δ	Δ	Δ	Δ	Δ	Δ	Δ	Δ	Δ	Δ	Δ	Δ	Δ	Δ

$$M_E = {}^9/_{51}$$

Δ	▲	Δ	▲	Δ	▲	Δ	▲	▲	Δ	Δ	Δ	Δ	Δ	Δ	Δ	Δ
Δ	▲	Δ	Δ	Δ	Δ	Δ	Δ	Δ	Δ	Δ	Δ	Δ	Δ	▲	Δ	Δ
▲	Δ	▲	Δ	Δ	Δ	Δ	Δ	Δ	Δ	Δ	Δ	Δ	Δ	Δ	Δ	Δ

$$M_E = {}^{12}/_{51}$$

▲	▲	Δ	▲	Δ	▲	Δ	▲	▲	Δ	Δ	Δ	Δ	▲	Δ	Δ	Δ
Δ	▲	Δ	Δ	Δ	Δ	Δ	Δ	Δ	Δ	Δ	Δ	Δ	Δ	Δ	Δ	Δ
▲	Δ	▲	▲	Δ	Δ	Δ	Δ	Δ	Δ	Δ	Δ	Δ	▲	Δ	Δ	Δ

Table 10: Comparison of the ED4 and ED17 reduced models for stress $\bar{\tau}_{xz}$ obtained via 3D equilibrium equations, symmetric cross-ply laminated plate (0°/90°/0°), $a/h = 4$ and $a/h = 20$.

$a/h = 4$			$a/h = 20$		
M_E	% Error – ED4	% Error – ED17	M_E	% Error – ED4	% Error – ED17
${}^5/_{51}$	4.5957	1.3234	${}^5/_{51}$	0.3387	0.0843
${}^8/_{51}$	4.5144	0.7569	${}^7/_{51}$	0.3162	0.0319
${}^{10}/_{51}$	4.5144	0.3842	${}^9/_{51}$	0.3162	0.0230
${}^{14}/_{51}$	4.5144	0.3525	${}^{12}/_{51}$	0.3162	0.0184

Table 11: Reduced ED17 models for stress $\bar{\sigma}_{xx}$, asymmetric cross-ply laminated plate (0°/90°), $a/h = 4$.

$$M_E = {}^{7}/_{51}$$

▲	▲	△	△	△	△	▲	△	△	△	△	△	△	△	△	△	△
▲	▲	△	△	△	△	△	△	△	△	△	△	△	△	△	△	△
▲	△	△	△	△	△	△	△	△	△	△	△	△	▲	△	△	△

$$M_E = {}^{9}/_{51}$$

▲	▲	△	△	▲	△	▲	△	△	△	△	△	△	▲	△	△	△
▲	▲	△	▲	△	△	△	△	△	△	△	△	△	△	△	△	△
▲	△	△	△	△	△	△	△	△	△	△	△	△	△	△	△	△

$$M_E = {}^{11}/_{51}$$

▲	△	▲	△	△	△	▲	△	△	△	△	△	△	▲	▲	△	△
△	▲	△	△	△	△	△	△	△	△	△	△	△	▲	△	△	▲
▲	△	△	△	△	△	△	△	△	△	△	▲	△	▲	△	△	△

$$M_E = {}^{13}/_{51}$$

▲	▲	▲	▲	▲	▲	△	▲	△	△	△	△	△	△	▲	△	△
▲	△	△	▲	△	▲	△	△	△	△	△	△	△	△	△	△	△
▲	▲	△	△	△	△	△	△	△	△	△	△	△	△	△	△	△

Table 12: Reduced ED17 models for stress $\bar{\sigma}_{xx}$, asymmetric cross-ply laminated plate (0°/90°), $a/h = 20$.

$$M_E = {}^{6}/_{51}$$

▲	▲	△	△	△	△	▲	△	△	△	△	△	△	△	△	△	△
▲	▲	△	△	△	△	△	△	△	△	△	△	△	△	△	△	△
▲	△	△	△	△	△	△	△	△	△	△	△	△	△	△	△	△

$$M_E = {}^{10}/_{51}$$

▲	▲	△	△	▲	△	▲	△	△	△	△	△	△	△	△	▲	△
▲	▲	△	△	△	△	▲	△	△	△	△	△	△	△	△	△	△
▲	▲	△	△	△	△	△	△	△	△	△	△	△	△	△	△	△

$$M_E = {}^{12}/_{51}$$

▲	▲	△	△	▲	△	▲	△	△	△	△	△	△	△	△	▲	▲
▲	▲	△	▲	△	△	▲	△	△	△	△	△	△	△	△	△	△
▲	▲	△	△	△	△	△	△	△	△	△	△	△	△	△	△	△

Table 13: Comparison of the ED4 and ED17 reduced models for the $\bar{\sigma}_{xx}$ stress, asymmetric cross-ply laminated plate (0°/90°), $a/h = 4$ and $a/h = 20$.

$a/h = 4$			$a/h = 20$		
M_E	% Error – ED4	% Error – ED17	M_E	% Error – ED4	% Error – ED17
$7/51$	2.2384	1.7480	$6/51$	0.1636	0.1036
$9/51$	1.9519	0.9017	$10/51$	0.0752	0.0491
$11/51$	1.8451	0.7336	$12/51$	0.0752	0.0343
$13/51$	1.8451	0.5488			

Table 14: Reduced ED17 models for stress $\bar{\sigma}_{xx}$, symmetric cross-ply laminated plate (0°/90°/90°/0°), $a/h = 4$.

$$M_E = {}^6/_{51}$$

Δ	▲	Δ	▲	Δ	▲	Δ	Δ	Δ	Δ	Δ	Δ	Δ	Δ	Δ	Δ	Δ
Δ	▲	Δ	▲	Δ	Δ	Δ	Δ	Δ	Δ	Δ	Δ	Δ	Δ	Δ	Δ	Δ
▲	Δ	Δ	Δ	Δ	Δ	Δ	Δ	Δ	Δ	Δ	Δ	Δ	Δ	Δ	Δ	Δ

$$M_E = {}^8/_{51}$$

▲	▲	Δ	▲	▲	Δ	Δ	Δ	Δ	Δ	Δ	Δ	Δ	Δ	▲	Δ	Δ
Δ	▲	Δ	▲	Δ	Δ	Δ	Δ	Δ	Δ	Δ	Δ	Δ	Δ	Δ	Δ	Δ
▲	Δ	Δ	Δ	Δ	Δ	Δ	Δ	Δ	Δ	Δ	Δ	Δ	Δ	Δ	Δ	Δ

$$M_E = {}^{10}/_{51}$$

Δ	▲	Δ	▲	▲	▲	Δ	Δ	Δ	Δ	Δ	Δ	Δ	Δ	▲	Δ	Δ
Δ	▲	Δ	▲	Δ	Δ	Δ	Δ	Δ	Δ	Δ	Δ	Δ	Δ	Δ	Δ	Δ
▲	▲	Δ	Δ	▲	Δ	Δ	Δ	Δ	Δ	Δ	Δ	Δ	Δ	Δ	Δ	Δ

$$M_E = {}^{12}/_{51}$$

Δ	▲	Δ	▲	▲	Δ	Δ	Δ	Δ	Δ	Δ	Δ	Δ	▲	Δ	▲	▲
Δ	▲	Δ	▲	Δ	Δ	Δ	Δ	Δ	Δ	Δ	Δ	Δ	Δ	Δ	Δ	Δ
▲	Δ	Δ	Δ	Δ	Δ	Δ	Δ	Δ	Δ	Δ	Δ	Δ	▲	Δ	▲	▲

$$M_E = {}^{15}/_{51}$$

Δ	▲	Δ	▲	▲	▲	▲	Δ	Δ	Δ	▲	▲	Δ	Δ	Δ	▲	▲
Δ	▲	Δ	▲	Δ	Δ	Δ	Δ	Δ	▲	Δ	Δ	Δ	Δ	Δ	Δ	Δ
▲	Δ	Δ	Δ	Δ	Δ	Δ	Δ	Δ	Δ	Δ	Δ	▲	Δ	▲	▲	

Table 15: Reduced ED17 models for stress $\bar{\sigma}_{xx}$, symmetric cross-ply laminated plate (0°/90°/90°/0°), $a/h = 20$.

$$M_E = {}^5/_{51}$$

△	▲	△	▲	△	▲	△	△	△	△	△	△	△	△	△	△	△
△	▲	△	△	△	△	△	△	△	△	△	△	△	△	△	△	△
▲	△	△	△	△	△	△	△	△	△	△	△	△	△	△	△	△

$$M_E = {}^8/_{51}$$

▲	▲	△	▲	▲	△	△	△	△	▲	△	△	△	△	▲	△	△
△	▲	△	△	△	△	△	△	△	△	△	△	△	△	△	△	△
▲	△	△	△	△	△	△	△	△	△	△	△	△	△	△	△	△

$$M_E = {}^{11}/_{51}$$

▲	▲	△	▲	▲	△	△	△	△	▲	△	△	△	▲	▲	△	▲
△	▲	△	△	△	△	△	△	△	△	△	△	△	△	△	△	△
▲	▲	△	△	△	△	△	△	△	△	△	△	△	△	△	△	△

$$M_E = {}^{15}/_{51}$$

▲	▲	▲	▲	▲	▲	▲	△	△	▲	△	△	△	▲	▲	▲	▲
△	▲	△	△	△	△	△	△	△	△	△	△	△	△	△	△	△
▲	▲	△	△	△	△	△	△	△	△	△	△	△	△	△	△	△

Table 16: Comparison of the ED4 and ED17 reduced models for the $\bar{\sigma}_{xx}$ stress, symmetric cross-ply laminated plate (0°/90°/90°/0°), $a/h = 4$ and $a/h = 20$.

$a/h = 4$			$a/h = 20$		
M_E	% Error – ED4	% Error – ED17	M_E	% Error – ED4	% Error – ED17
${}^6/_{51}$	2.2269	1.7579	${}^5/_{51}$	0.2288	0.1828
${}^8/_{51}$	2.0127	1.4442	${}^8/_{51}$	0.2173	0.1046
${}^{10}/_{51}$	1.9397	1.0326	${}^{11}/_{51}$	0.2173	0.0742
${}^{12}/_{51}$	1.9397	0.7753	${}^{15}/_{51}$	0.2173	0.0462
${}^{15}/_{51}$	1.9397	0.6372			

Table 17: Reduced ED17 models for stress $\bar{\tau}_{xz}$ obtained via 3D equilibrium equations, symmetric cross-ply laminated plate (0°/90°/90°/0°), $a/h = 4$.

$$M_E = {}^{6}/_{51}$$

Δ	▲	Δ	▲	Δ	▲	Δ	Δ	Δ	Δ	Δ	Δ	Δ	Δ	Δ	▲	Δ
Δ	▲	Δ	Δ	Δ	Δ	Δ	Δ	Δ	Δ	Δ	Δ	Δ	Δ	Δ	Δ	Δ
▲	Δ	Δ	Δ	Δ	Δ	Δ	Δ	Δ	Δ	Δ	Δ	Δ	Δ	Δ	Δ	Δ

$$M_E = {}^{9}/_{51}$$

Δ	▲	Δ	▲	▲	▲	Δ	Δ	Δ	Δ	Δ	Δ	Δ	Δ	▲	Δ	Δ
Δ	▲	Δ	Δ	Δ	Δ	▲	Δ	Δ	Δ	Δ	Δ	Δ	Δ	Δ	Δ	Δ
▲	Δ	Δ	Δ	Δ	Δ	Δ	Δ	Δ	Δ	Δ	Δ	Δ	▲	Δ	Δ	Δ

$$M_E = {}^{11}/_{51}$$

▲	▲	Δ	▲	▲	Δ	Δ	Δ	Δ	Δ	Δ	Δ	Δ	Δ	Δ	▲	▲
Δ	▲	Δ	▲	Δ	Δ	Δ	Δ	Δ	Δ	Δ	Δ	Δ	Δ	▲	Δ	Δ
▲	Δ	Δ	Δ	Δ	Δ	Δ	Δ	Δ	Δ	Δ	Δ	Δ	▲	Δ	Δ	Δ

$$M_E = {}^{15}/_{51}$$

▲	▲	▲	Δ	▲	▲	Δ	Δ	Δ	Δ	▲	Δ	Δ	▲	▲	Δ	▲
Δ	▲	Δ	▲	Δ	Δ	Δ	Δ	Δ	Δ	Δ	Δ	Δ	Δ	Δ	Δ	Δ
▲	Δ	▲	▲	Δ	Δ	Δ	Δ	Δ	Δ	Δ	Δ	Δ	▲	Δ	Δ	Δ

Table 18: Reduced ED17 models for stress $\bar{\tau}_{xz}$ obtained via 3D equilibrium equations, symmetric cross-ply laminated plate (0°/90°/90°/0°), $a/h = 20$.

$$M_E = {}^{5}/_{51}$$

Δ	▲	Δ	▲	Δ	▲	Δ	Δ	Δ	Δ	Δ	Δ	Δ	Δ	Δ	Δ	Δ
Δ	▲	Δ	Δ	Δ	Δ	Δ	Δ	Δ	Δ	Δ	Δ	Δ	Δ	Δ	Δ	Δ
▲	Δ	Δ	Δ	Δ	Δ	Δ	Δ	Δ	Δ	Δ	Δ	Δ	Δ	Δ	Δ	Δ

$$M_E = {}^{7}/_{51}$$

Δ	▲	Δ	▲	Δ	▲	Δ	Δ	Δ	Δ	Δ	Δ	Δ	Δ	Δ	Δ	Δ
Δ	▲	Δ	Δ	Δ	Δ	Δ	Δ	Δ	Δ	Δ	Δ	Δ	Δ	Δ	Δ	Δ
▲	Δ	▲	Δ	Δ	Δ	Δ	Δ	Δ	Δ	Δ	Δ	Δ	Δ	▲	Δ	Δ

$$M_E = {}^{9}/_{51}$$

▲	▲	Δ	▲	▲	Δ	Δ	Δ	Δ	▲	Δ	Δ	Δ	Δ	▲	Δ	Δ
Δ	▲	Δ	Δ	Δ	Δ	Δ	Δ	Δ	Δ	Δ	Δ	Δ	Δ	Δ	Δ	Δ
▲	Δ	▲	Δ	Δ	Δ	Δ	Δ	Δ	Δ	Δ	Δ	Δ	Δ	Δ	Δ	Δ

$$M_E = {}^{11}/_{51}$$

▲	▲	Δ	▲	▲	Δ	Δ	Δ	Δ	▲	▲	Δ	Δ	Δ	▲	Δ	Δ
Δ	▲	Δ	Δ	Δ	Δ	Δ	Δ	Δ	Δ	Δ	Δ	Δ	Δ	Δ	Δ	Δ
▲	Δ	▲	Δ	Δ	Δ	Δ	Δ	Δ	Δ	Δ	Δ	Δ	▲	Δ	Δ	Δ

Table 19: Comparison of the ED4 and ED17 reduced models for stress $\bar{\tau}_{xz}$ obtained via 3D equilibrium equations, symmetric cross-ply laminated plate (0°/90°/90°/0°), $a/h = 4$ and $a/h = 20$.

$a/h = 4$			$a/h = 20$		
M_E	% Error – ED4	% Error – ED17	M_E	% Error – ED4	% Error – ED17
$6/51$	2.0131	1.4448	$5/51$	0.1565	0.1163
$9/51$	1.9078	1.1294	$7/51$	0.1471	0.0876
$11/51$	1.8999	0.4819	$9/51$	0.1441	0.0372
$15/51$	1.8999	0.3643	$11/51$	0.1441	0.0282

Figures

Figure 1. Plate geometry and reference system.
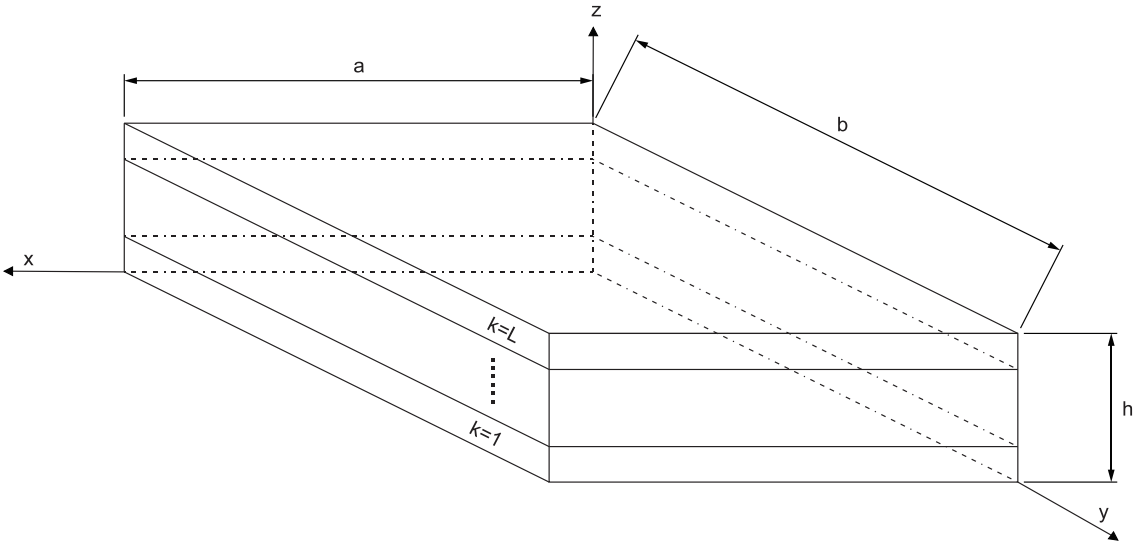
Figure 2. Displacement field of a refined model and genes of a chromosome.
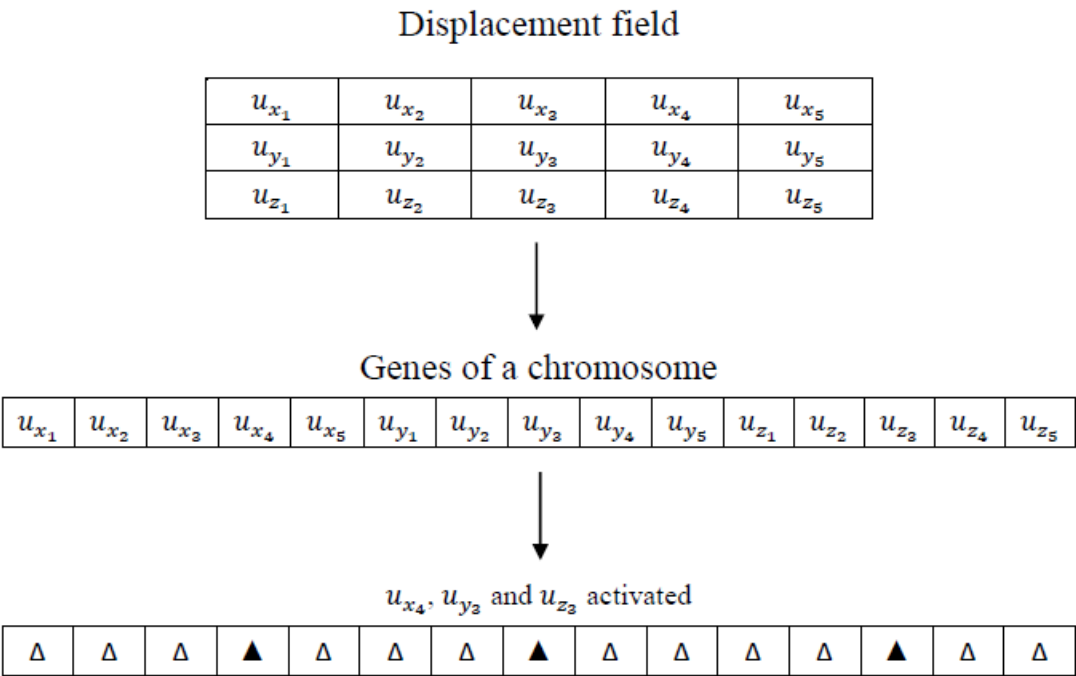
Figure 3. BTD based on ED4, cross-ply laminated plate (0°/90°/0°), $\bar{\sigma}_{xx}$, $^a/_h = 4$.
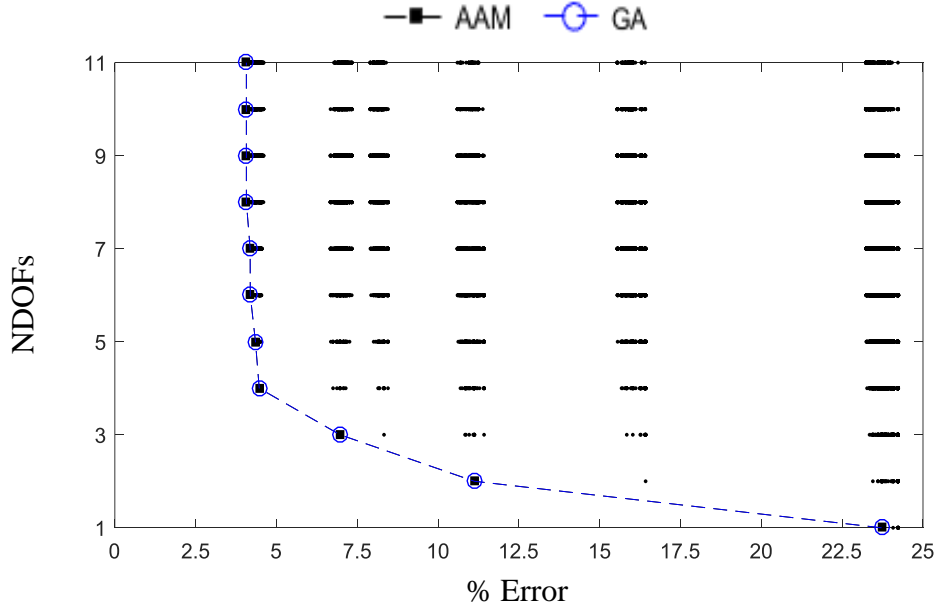
Figure 4. BTDs for a symmetric cross-ply laminated plate (0°/90°/0°), stress $\bar{\sigma}_{xx}$, (a) $^a/_h$ = 4, (b) $^a/_h$ = 20. The reduced polynomial ED4 models are built via the AAM (AAM – Pol) and the reduced Hybrid ED17 models are built via the genetic algorithm (GA - Hybrid).
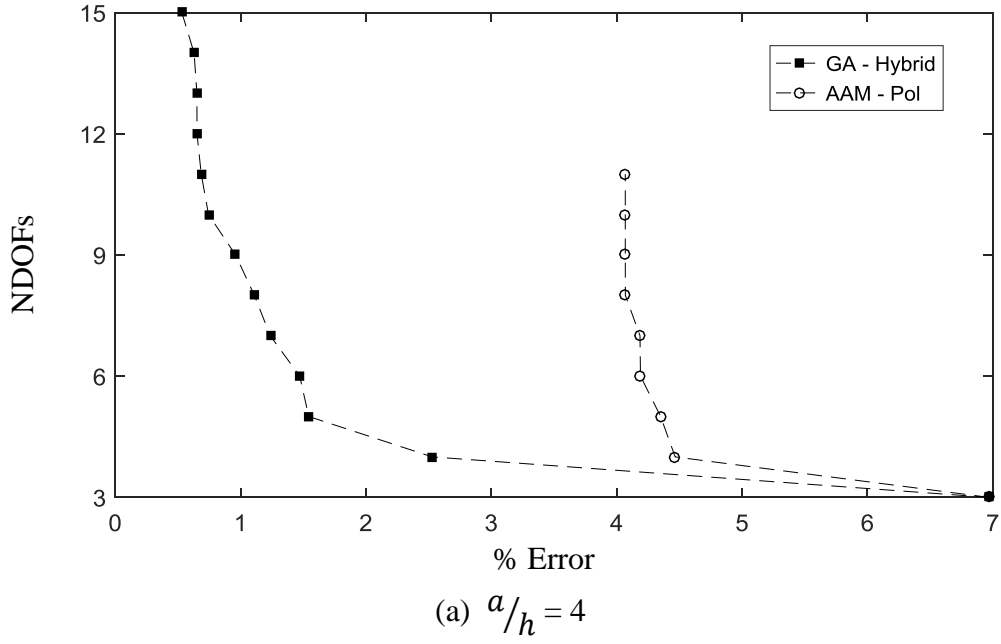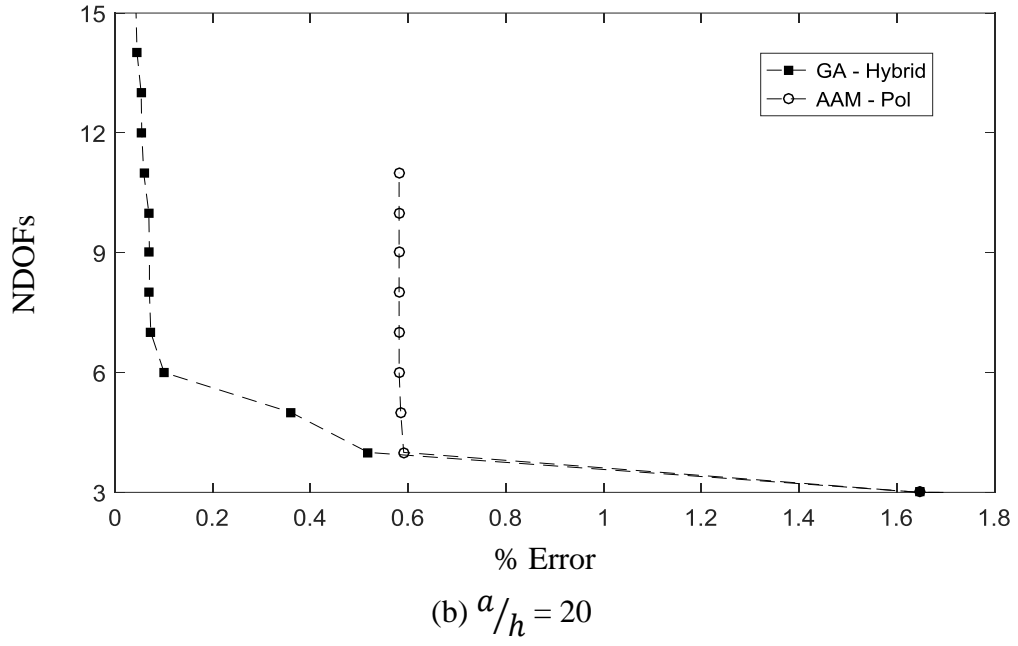
(a) $^a/_h = 4$

(b) $^a/_h = 20$

Figure 5. $\bar{\sigma}_{xx}$ distribution along the thickness of a symmetric cross-ply laminated plate (0º/90º/0º), (a) $^a/_h = 4$, (b) $^a/_h = 20$.
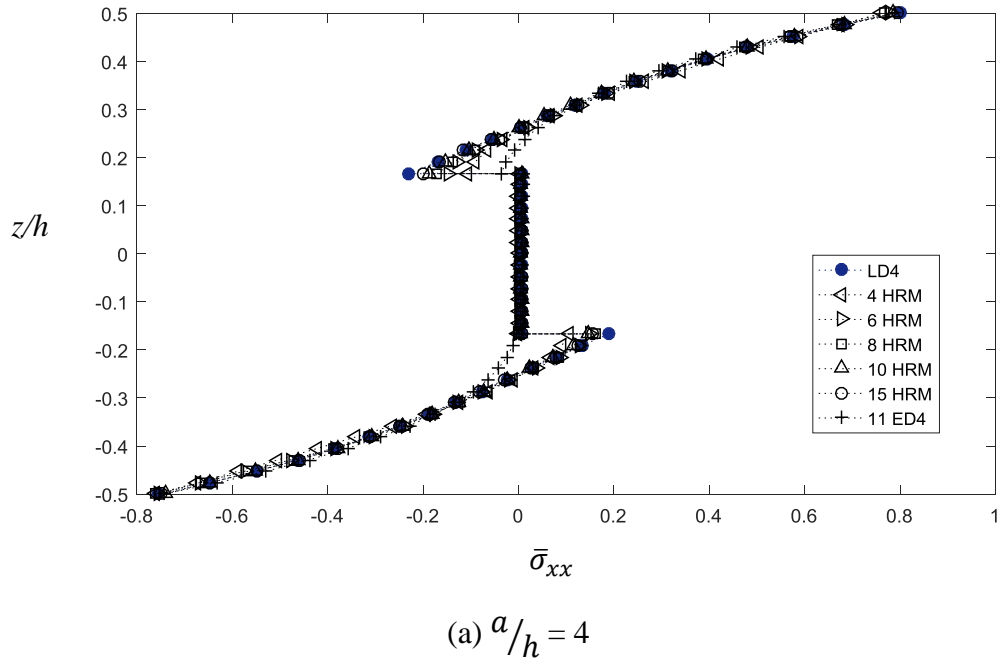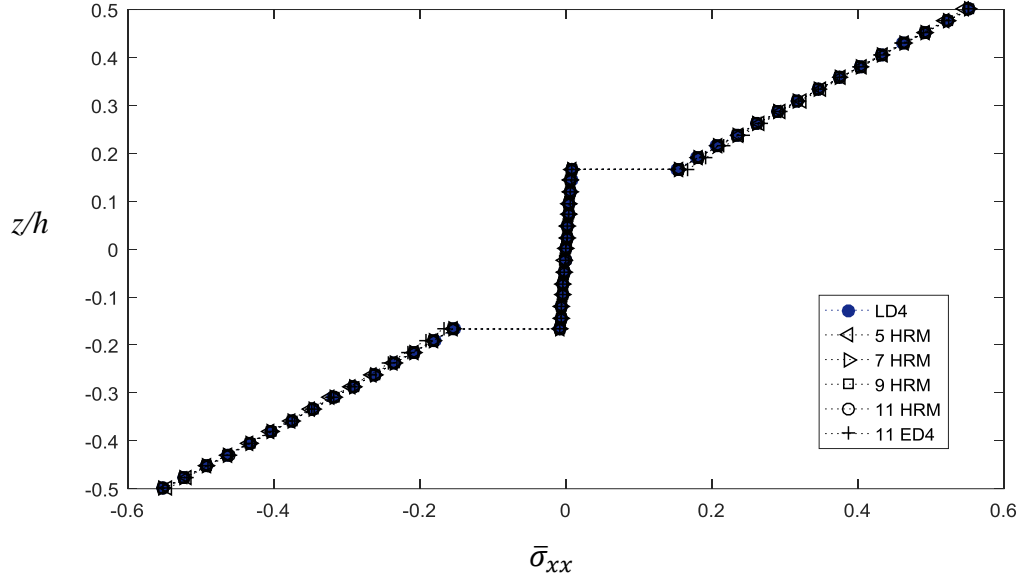
(a) $^a/_h = 4$

(b) $a/h = 20$
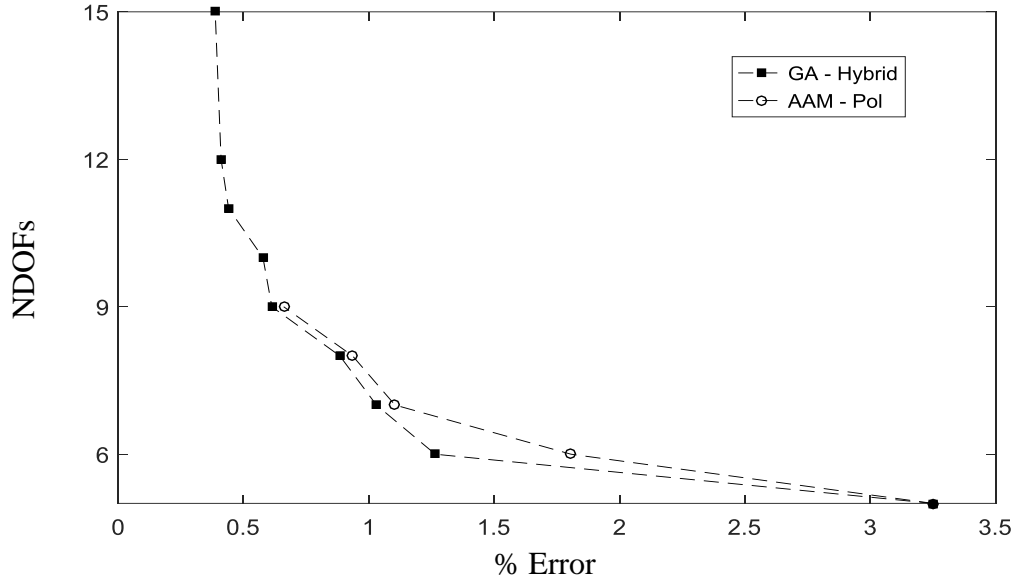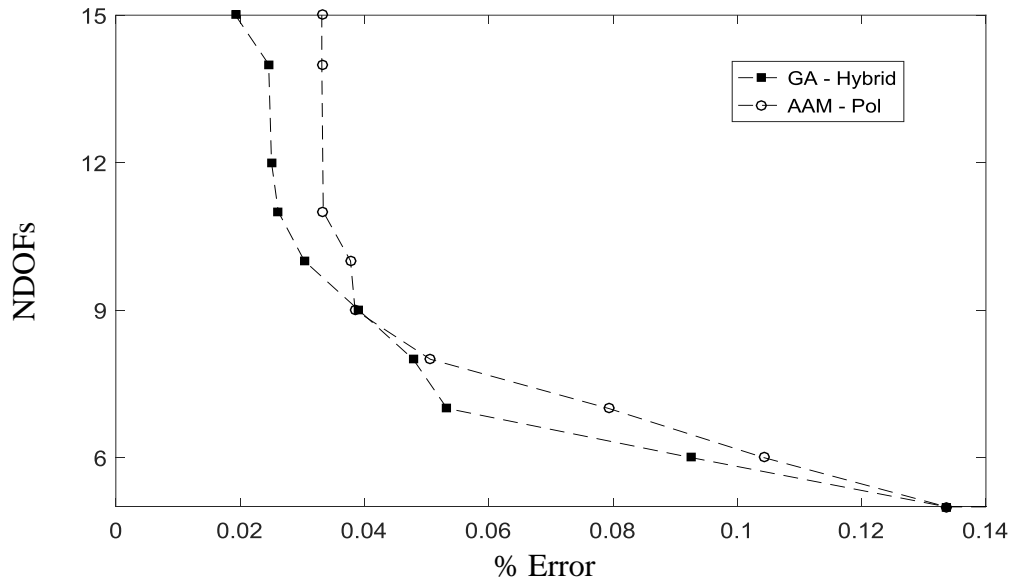
Figure 6. BTDs for a symmetric cross-ply laminated plate (0°/90°/0°), stress $\bar{\tau}_{xz}$ obtained via 3D equilibrium equations, (a) $a/h = 4$, (b) $a/h = 20$. The reduced polynomial ED4 models are built via the AAM (AAM − Pol) and the reduced Hybrid ED17 models are built via the genetic algorithm (GA - Hybrid).
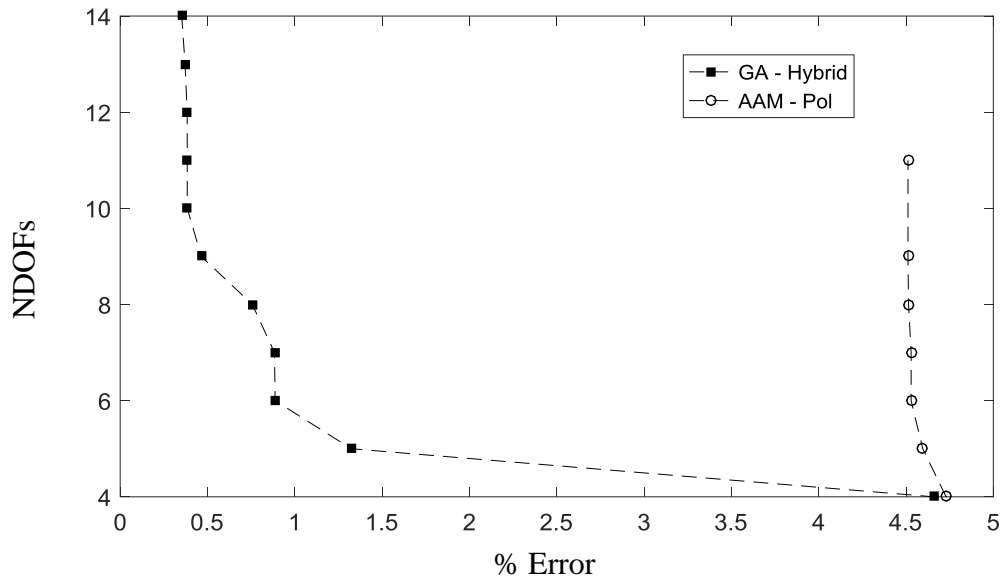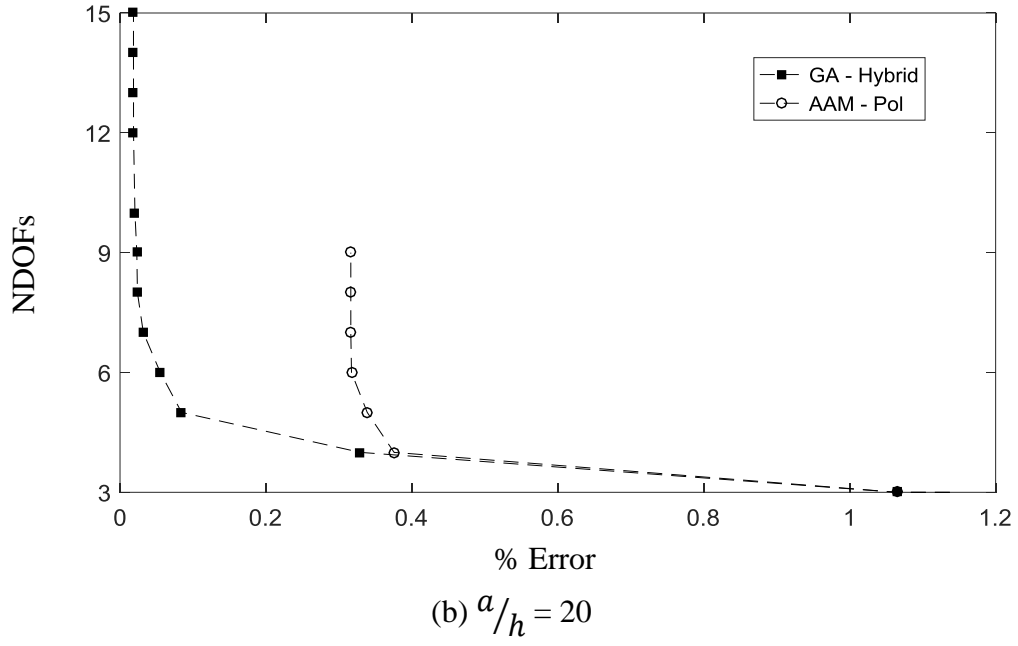
(a) $a/h = 4$

(b) $a/h = 20$

Figure 7. $\bar{\tau}_{xz}$ distribution along the thickness of a symmetric cross-ply laminated plate (0º/90º/0º) obtained via 3D equilibrium equations, (a) $a/h = 4$, (b) $a/h = 20$.
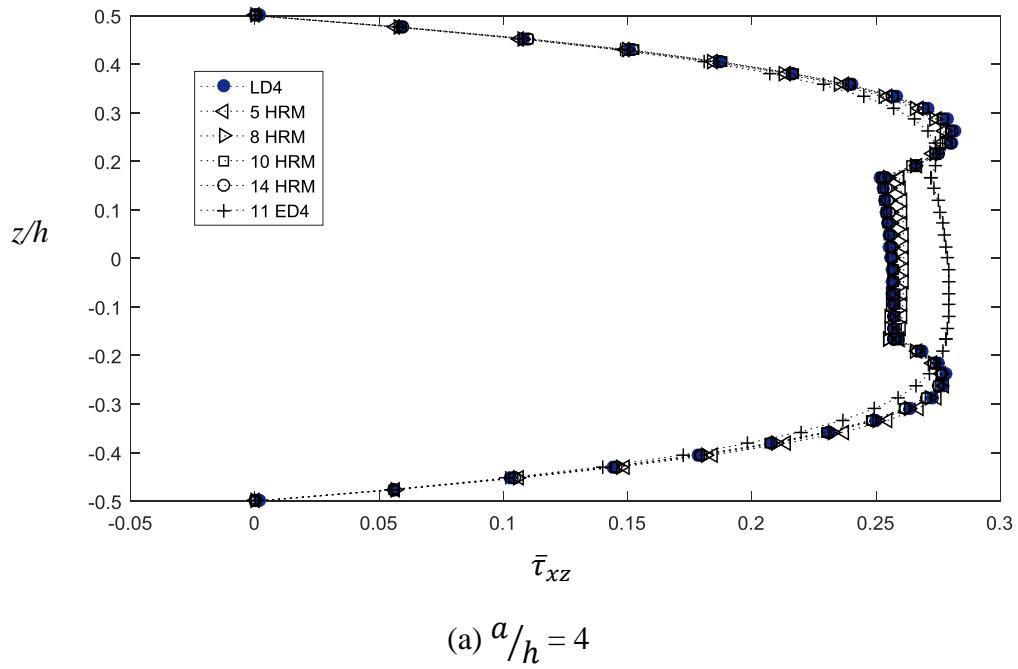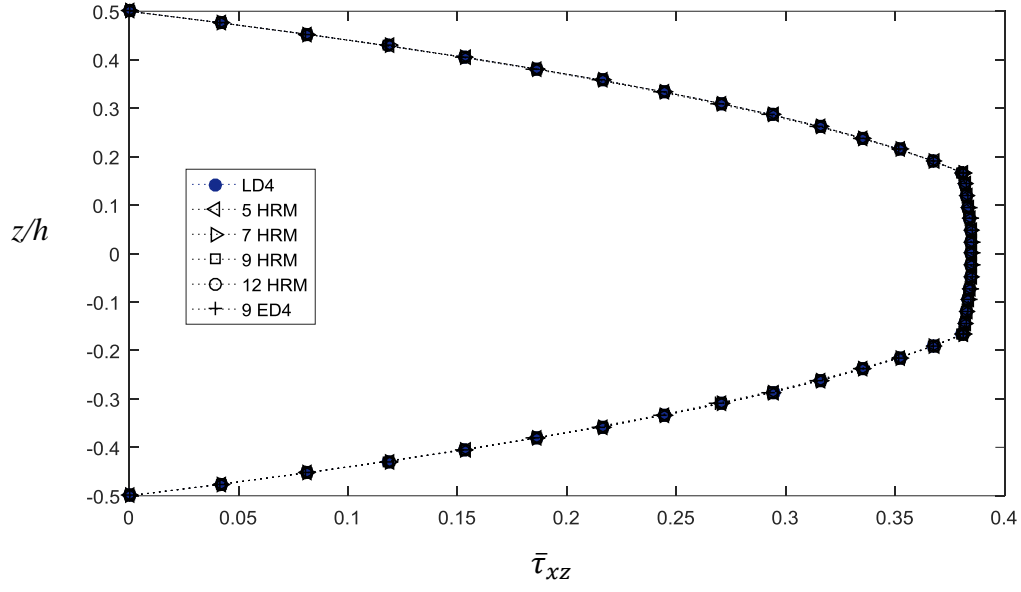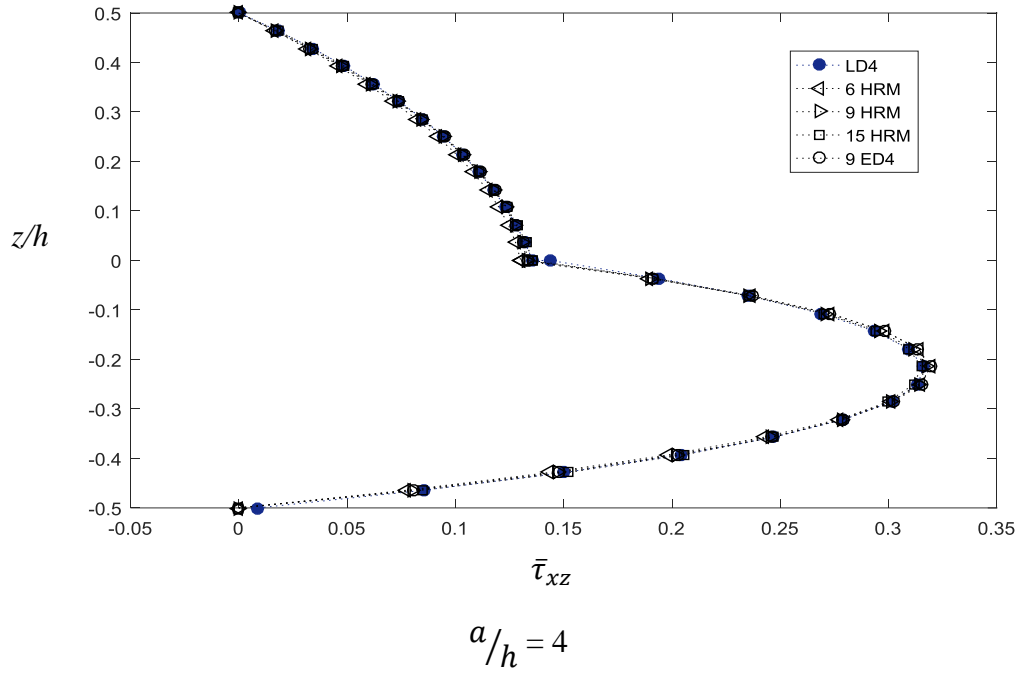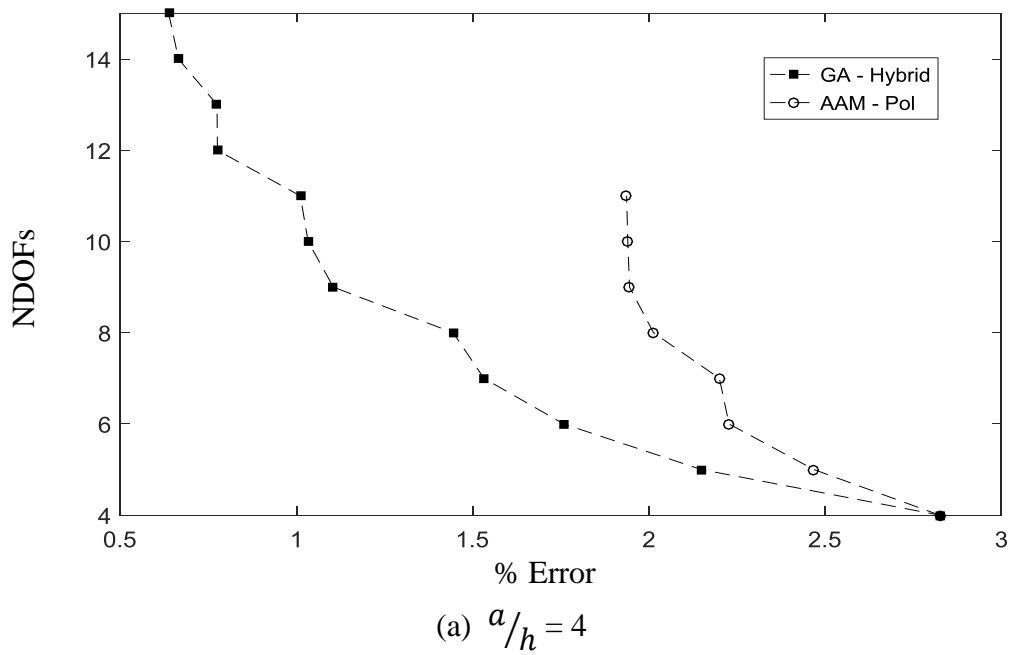

(a) $a/h = 4$

(b) $a/h = 20$

Figure 8. BTDs for an asymmetric cross-ply laminated plate (0°/90°), stress $\bar{\sigma}_{xx}$, (a) a/h = 4, (b) a/h = 20. The reduced polynomial ED4 models are built via the AAM (AAM − Pol) and the reduced Hybrid ED17 models are built via the genetic algorithm (GA - Hybrid).
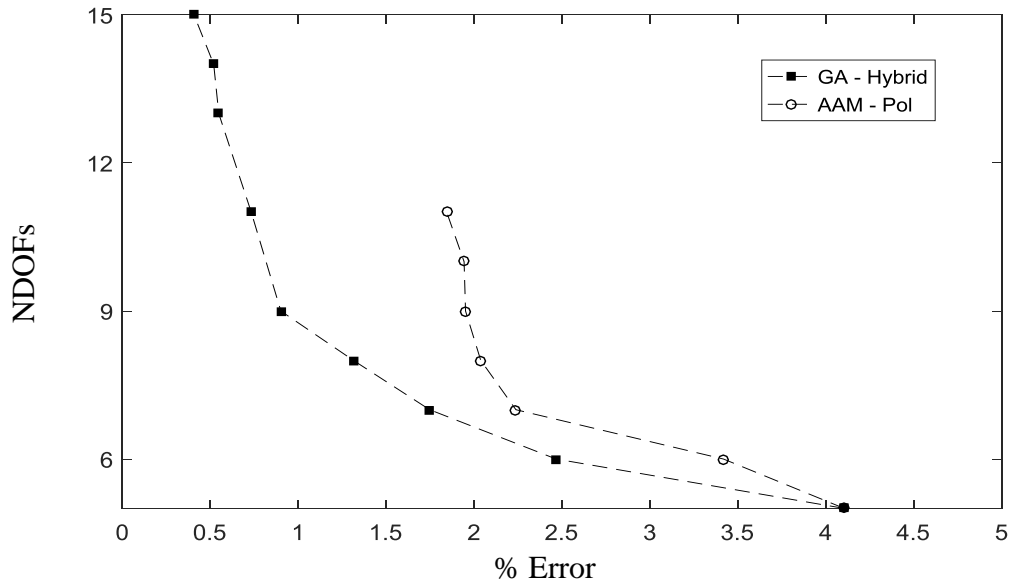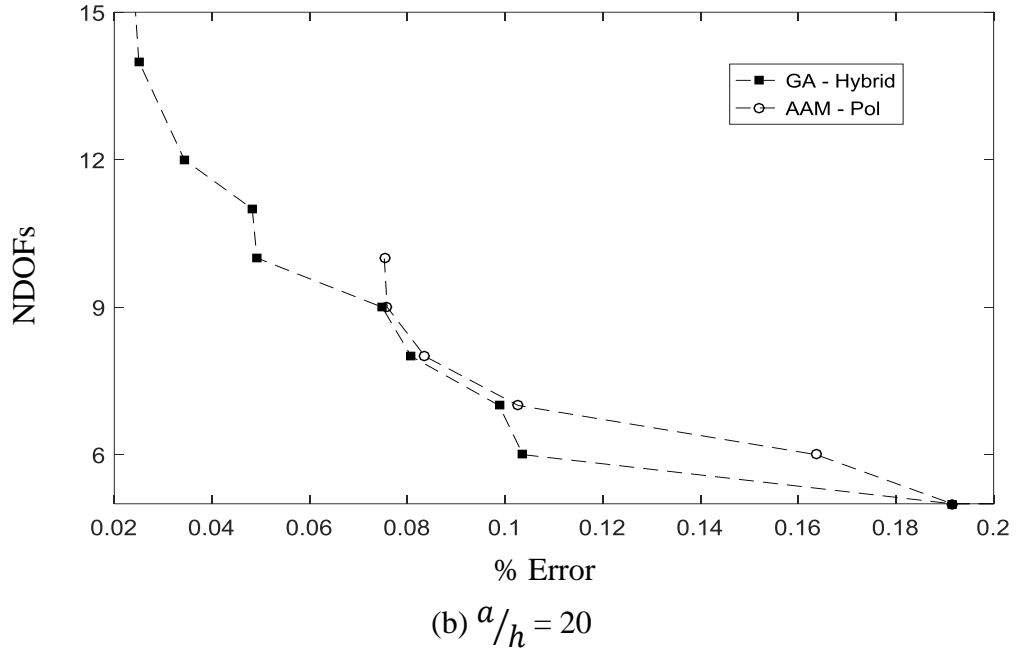
(a) $a/h = 4$

(b) $^a/_h = 20$

Figure 9. $\bar{\sigma}_{xx}$ distribution along the thickness of an asymmetric cross-ply laminated plate (0º/90º), $^a/_h = 4$.

$^a/_h = 4$
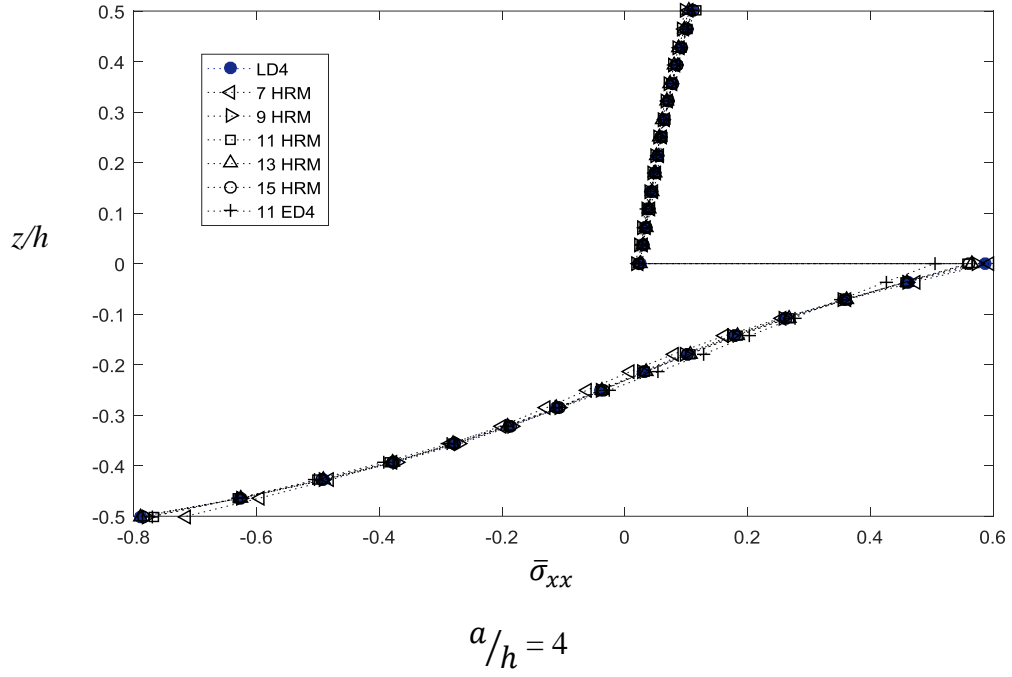
Figure 10. BTDs for an asymmetric cross-ply laminated plate (0º/90º), stress $\bar{\tau}_{xz}$ obtained via 3D equilibrium equations, (a) $a/h = 4$, (b) $a/h = 20$. The reduced polynomial ED4 models are built via the AAM (AAM – Pol) and the reduced Hybrid ED17 models are built via the genetic algorithm (GA - Hybrid).
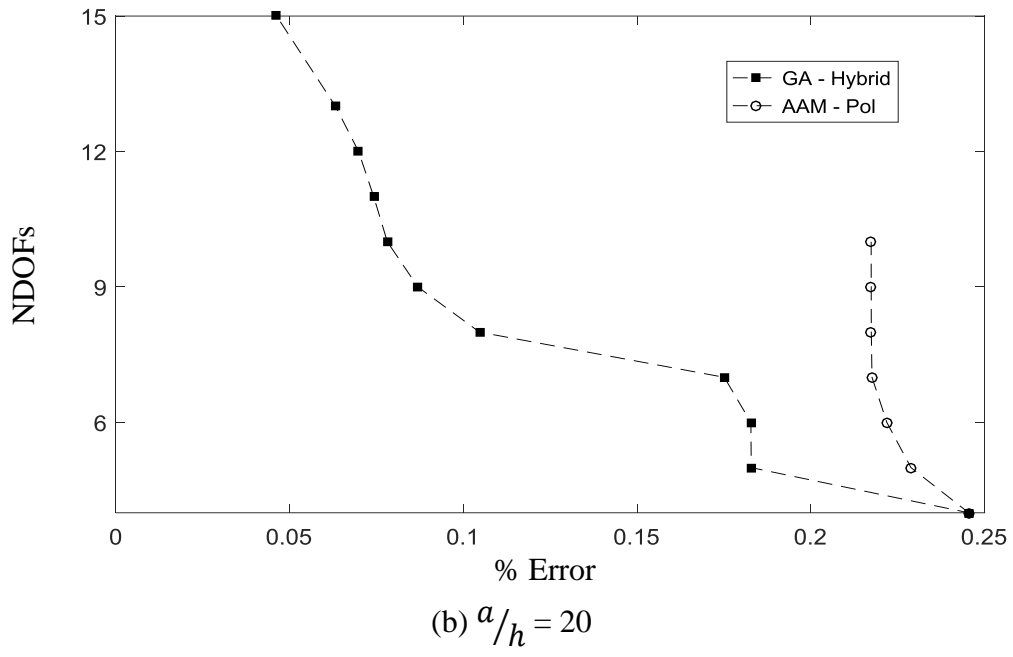

(a) $a/h = 4$

(b) $a/h = 20$

Figure 11. $\bar{\tau}_{xz}$ distribution along the thickness of an asymmetric cross-ply laminated plate (0º/90º) obtained via 3D equilibrium equations, $a/h = 4$.

$a/h = 4$

Figure 12. BTDs for a symmetric cross-ply laminated plate (0º/90º/90º/0º), stress $\bar{\sigma}_{xx}$, (a) $a/h = 4$, (b) $a/h = 20$. The reduced polynomial ED4 models are built via the AAM (AAM – Pol) and the reduced Hybrid ED17 models are built via the genetic algorithm (GA - Hybrid).

(a) $a/h = 4$

43

(b) $a/h = 20$

Figure 13. $\bar{\sigma}_{xx}$ distribution along the thickness of a symmetric cross-ply laminated plate (0º/90º/90º/0º), $a/h = 4$.

$a/h = 4$

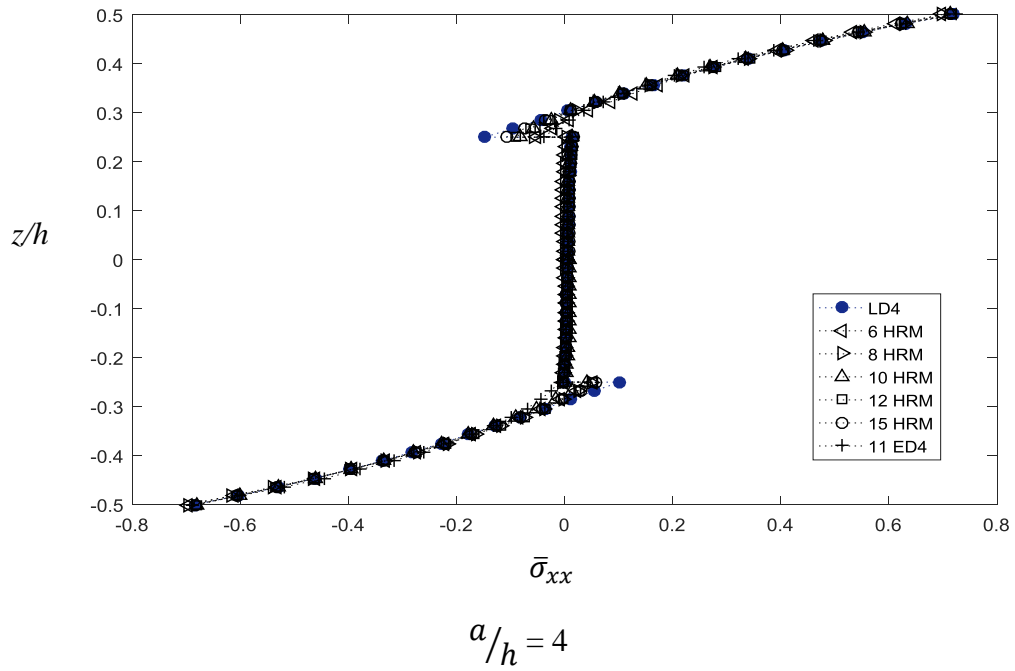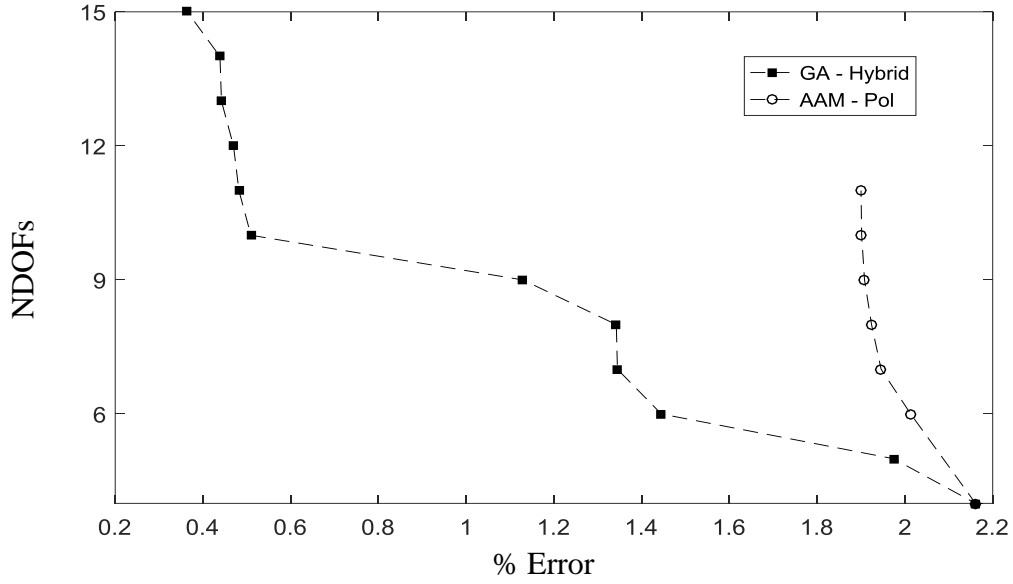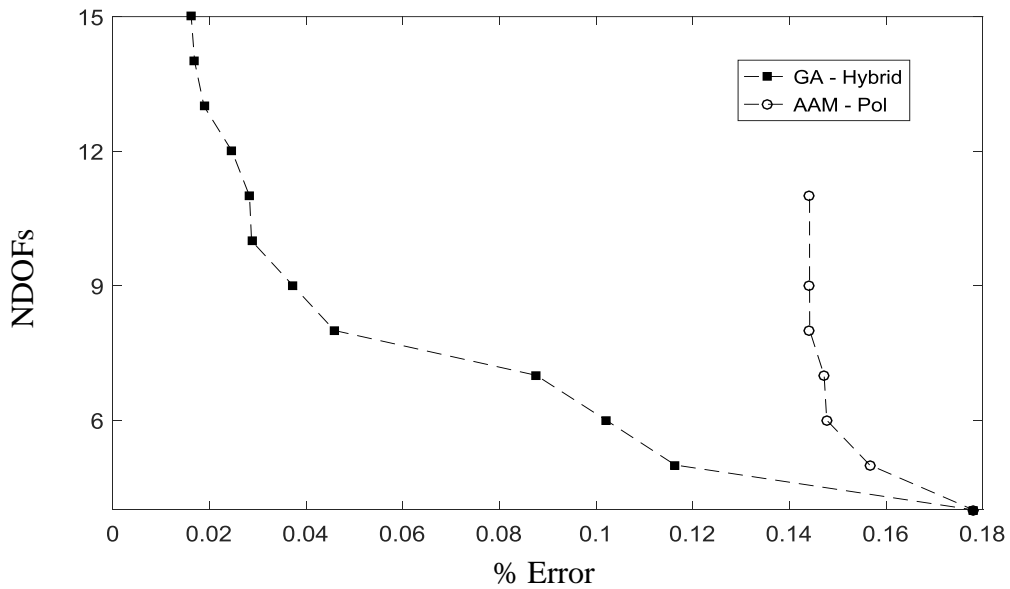Figure 14. BTDs for a symmetric cross-ply laminated plate (0º/90º/90º/0º), stress $\bar{\tau}_{xz}$ obtained via 3D equilibrium equations, (a) $a/h = 4$, (b) $a/h = 20$. The reduced polynomial ED4 models are built via the AAM (AAM – Pol) and the reduced Hybrid ED17 models are built via the genetic algorithm (GA - Hybrid).

(a) $a/h = 4$

(b) $a/h = 20$

Figure 15. $\bar{\tau}_{xz}$ distribution along the thickness of a symmetric cross-ply laminated plate (0º/90º/90º/0º) obtained via 3D equilibrium equations, $a/h = 4$.

$$a/h = 4$$